Supplementary material

Engineered Amine Oxidase for Efficient Oxidative Dehydroaromatization of 1,2,3,4-Tetrahydroquinolines toward Quinolines in Aqueous Media

Mengmeng He,[a] Xiaoyang Yue,*[a][b] Jianqiao Liu,[a][b] Guanhua Liu, [a][b] Liya Zhou, [a][b] Ying He, [a][b] Li Ma, [a][b] Yunting Liu*[a][b] and Yanjun Jiang*[a][b]

[a] School of Chemical Engineering and Technology, Hebei University of Technology, Tianjin 300401, China

[b] National-Local Joint Engineering Laboratory for Energy Conservation in Chemical Process Integration and Resources Utilization, Hebei University of Technology, Tianjin 300401, China

*E-mail: xiaoyang.yue@hebut.edu.cn;
*E-mail: ytliu@hebut.edu.cn;
*E-mail: yanjunjiang@hebut.edu.cn

Contents

Chemicals and materials

All chemicals and reagents were purchased from commercial suppliers (MREDA, Kermel, Aladdin, Macklin, Solarbio and Sangon Biotech) at least of reagent grade and used without further purification unless otherwise noted. Potassium phosphate buffer (50 mM, pH=7.5) was used as a buffering system unless otherwise specified. *E. coli* BL21 (DE3) cells were grown using Luria–Bertani (LB) medium. pET-28a (+) was used as the cloning and expression vector for all enzymes described in this study.

Enzyme library mining

The candidate enzymes were mined by BLAST in NCBI database using MAO5 as template. Then, the sequences with identity less than 30% and more than 80% were removed. The physical and chemical properties of candidates, for instance, molecular weight, theoretical pI, amino acid composition, atomic composition, extinction coefficient, estimated half-life, instability index, aliphatic index and grand average of hydropathicity of proteins can be estimated in this database only by inputting the protein sequence, were estimated using online database Expasy (https://web.expasy.org/protparam/). The solubility of the candidates was estimated using Protein-Sol (https://protein-sol.manchester.ac.uk/)[1] and the genes which were estimated by the program Protein-Sol to be insolubly expressed in *E. coli* were eliminated. Multiple sequence alignments were performed using the MEGA server (https://www.megasoftware.net/show_eua) and displayed using ESPript (https://espript.ibcp.fr/ESPript/ESPript/index.php). 6 sequences from each branch were selected for gene synthesis and characterization. The protein sequences encoding candidate enzymes and model enzyme (Supporting Information, Table S1) were codon-optimized and chemically synthesized (Sangon Biotech, China). The candidate amine oxidase genes from *Gammaproteobacteria bacterium, Pseudomonas* sp.*, Saccharospirillum* sp.*, Thalassomonas* sp. RHCI1, *Luminiphilus* sp. *and Vibrio* sp. JCM 19236. All enzyme genes were inserted into the expression vector pET-28a (+) and subsequently transformed into *E. coli* BL21 (DE3) for expression.

Protein expression and purification of model enzyme and candidate enzymes

Recombinant *E. coli* BL21 (DE3) strain were cultured in 10 mL LB medium containing 50 μg/mL kanamycin (final concentration) at 37°C and 200 rpm overnight. Then, 0.5 mL preculture was inoculated in 50 mL TB medium with 50 μg/mL kanamycin, cultured at 37°C and 200 rpm until OD600 reached 0.6~0.8, and then induced by addition of IPTG (final concentration of 0.2 mM) at 25°C for further 20 h. After medium removal by centrifugation (8000 rpm, 5 min, 4°C), the cell pellets were washed with potassium phosphate buffer (50 mM, pH 7.5) twice and resuspended in the same buffer. The cells were disrupted by high-pressure homogenization, and cell debris was removed by centrifugation (10000 rpm, 20 min, 4°C). Unless otherwise stated, the crude lysate in this study was obtained by this method. The crude lysates were used for SDS-PAGE analysis.

Ni-NTA affinity chromatography was performed to purify the filtered lysate. After pre-equilibrating the Ni-NTA column with buffer A (20 mM NaH_2PO_4, 500 mM NaCl, and 20 mM imidazole at pH 7.4), the filtered lysate was loaded into the Ni-NTA column. Subsequently, bound protein was recovered with gradient elution buffer (20 mM NaH_2PO_4, 500 mM NaCl, pH 7.4) containing 30 mM, 60 mM, 300 mM and 500 mM imidazole for 5-10 column volumes, respectively. Fractions containing target protein was verified by SDS-PAGE analysis and concentrated by ultrafiltration.

Enzyme library screening

Reaction mixture comprising potassium phosphate buffer (50 mM, pH 7.5), substrate 1a (5 mM), purified AOs (2.0 mg/mL), in a total volume of 5 mL was incubated at 37°C with 200 rpm shaking for 24 h. The sample was then analyzed by HPLC method.

Mutagenesis

The site-directed mutagenesis was conducted using recombinant plasmids containing *Vs*AO genes (Table S6) as templates with the following program: 98 ℃ for 5 min, (98 ℃ for 2 min, 55 ℃ for 30 s, 68 ℃ for 60 s) with 15 cycles, 68 ℃ for 5 min 4 ℃ hold. 50 μL PCR reaction mixture contains reverse upstream and downstream primers (1.5 μL each), 2 μL recombinant plasmid, 25 μL K_{OD} DNA Polymerase and 20 μL distilled water. The PCR products were digested by *NcoI* and *XhoI*, and transformed into *E. coli*. BL21 (DE3) cells. The sequences were verified by DNA sequencing, and the oxidative dehydroaromatization activity of developed *Vs*AO variants was detected via HPLC method. The primers used in this work are shown in Table S7.

Enzymatic properties of *Vs*AO

The effect of pH on enzyme activity was determined at diverse pH levels (5.0–10.5) in the following buffers (50 mM): Citrate buffer (pH 5.0, 5.5, 6.0), potassium phosphate buffer (pH 6.0, 6.5, 7.0, 7.5, 8.0) and Gly-NaOH buffer (pH 8.0, 8.5, 9.0, 9.5, 10.0, 10.5). The pH stability of *Vs*AO was determined by preincubating the purified *Vs*AO in different pH (7.5, 10.0) buffers, followed by measuring the residual activity at 37°C. The effect of temperature on enzyme activity was determined at different temperatures ranging from 20 to 70°C. The thermostability of *Vs*AO was determined by preincubating the purified *Vs*AO at different temperatures (30°C, 50°C) followed by measuring the residual activity at 30°C. The highest enzyme activity was taken as 100%.

Enzymatic properties of M2

The effect of pH on enzyme activity was determined at diverse pH levels (4.0–11.0) in the following buffers (50 mM): Citrate buffer (pH 4.0, 4.5, 5.0, 5.5, 6.0), potassium phosphate buffer (pH 6.0, 6.5, 7.0, 7.5, 8.0) and Gly-NaOH buffer (pH 8.0, 8.5, 9.0, 9.5, 10.0, 10.5, 11.0). The pH stability of M2 was determined by preincubating the purified M2 in different pH (7.5, 10.0) buffers, followed by measuring the residual activity at 30°C. The effect of temperature on enzyme activity was determined at different temperatures ranging from 20 to 70°C. The thermostability of M2 was determined by preincubating the purified M2 at different temperatures (35℃, 50°C) followed by measuring the residual activity at 30°C. The highest enzyme activity was taken as 100%.

Enzyme activity assay

The activities of *Vs*AO were measured by HPLC at 254 nm. The activity assay was carried out in 1 mL reaction mixture containing potassium phosphate buffer (50 mM, pH 7.5), substrate **1a** (5 mM) and appropriate purified enzyme solution at 30℃. 1 U was defined as the amount of enzyme required to catalyze the conversion of 1 μmol of substrate per minute under specified assay conditions.

Molecular docking

AutoDock 4 was used for the docking of substrate 1a into the predicted structures. A grid box of 8 × 8 × 8 with spacing of 1.0 Å, which encompassed the active sites of *Vs*AO, was set as the search space to explore suitable substrate-binding modes. The PDBQT format was employed for both the input and output of molecular structures.

Determination of kinetic parameters

Purified *Vs*AO and its mutants were kinetically characterized to determine Michaelis Menten-parameters for oxidative dehydroaromatization of 2-methyl-1,2,3,4-tetrahydroquinoline (2-MeTHQ, **1a**). The substrate concentrations were varied from 0.5-10 mM while keeping the other reaction conditions same. Reactions were performed at 30°C in 1 mL volume and contained 50 mM potassium phosphate buffer (pH 7.5), substrate **1a** and appropriate purified enzyme solution. Due to limited substrate solubility, activity at higher concentrations could not be explored.

Time-course experiments

The oxidative dehydroaromatization reaction of **5a** was carried out in a 1000 mL three-neck flask equipped with a magnetic stirrer. Substrate **5a** (756 mg, 5 mmol) was initially dissolved in 50 mL of DMSO as substrate solution. Then, 50 mL of substrate solution and freeze-dried whole cells containing *Vs*AO or M2(16 g/L) was added to 450 mL of the potassium phosphate buffer (50 mM, pH=7.5). The final concentration of substrate **5a** was 10 mM in the reaction. The pH condition was kept at 7.5 and a thermostat-controlled water bath was used to maintain the reaction at 30°C. The reaction was monitored by HPLC.

Preparative-scale oxidative dehydroaromatization of 5a and 18b

The preparative-scale oxidative dehydroaromatization reaction of **5a** and **18a** was carried out in a 1000 mL three-neck flask equipped with a magnetic stirrer. Substrate **5a** (756 mg, 5 mmol) or **18a** (838 mg, 5 mmol) was initially dissolved in 50 mL of DMSO as substrate solution. Then, 50 mL of substrate solution and freeze-dried whole cells containing M2(16 g/L) was added to 450 mL of the potassium phosphate buffer (50 mM, pH=7.5). The final concentration of substrate **5a** and **18a** was 10 mM in the reaction. The pH condition was maintained at 7.5 and a thermostat-controlled water bath was used to keep the reaction at 30°C. The reaction was monitored by HPLC. Upon the completion of the reactions, 500 mL of samples was collected, 1500 mL of ethyl acetate was added, and the organic layers were dried over $MgSO_4$ and filtered. The residue was purified by column chromatography using a gradient of hexane and ethyl acetate. The mixture was concentrated so that products **5b** and **18b** was obtained and analyzed using NMR, as described in the ESI.

Analytical methods

Method 1 HPLC was performed with a Daicel Chiralcel OJ-H column (n-hexane/isopropanol mixtures as solvent) or Daicel Chiralcel AD column (n-hexane/isopropanol/diethylamine mixtures as solvent) at 30°C at 254 nm UV detector.

Method 2 ^{1}H NMR and ^{13}C NMR spectra were recorded on a Bruker AV 400 spectrometer at 400 MHz with $CDCl_3$/DMSO-d6 as solvent. Chemical shifts were reported in ppm relative to internal TMS for ^{1}H NMR data, respectively. Data are presented in the following space: chemical shift, multiplicity, coupling constant in hertz (Hz), and signal area integration in natural numbers.

Supplementary Data

The phylogenetic tree of amine oxidases

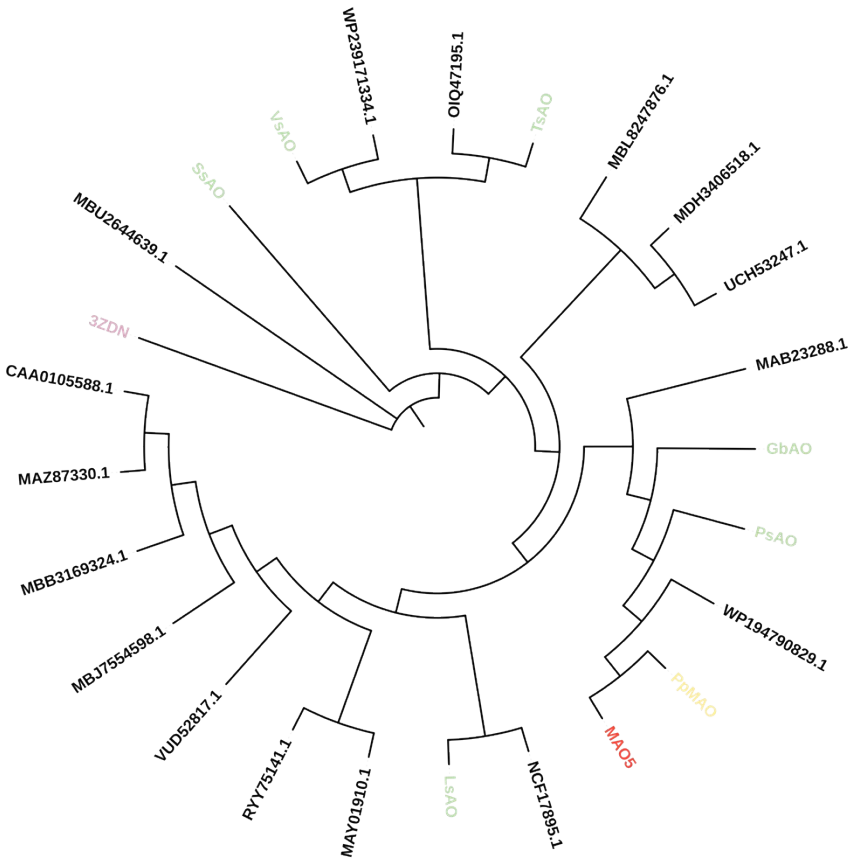

Figure S1. The phylogenetic tree of amine oxidases used in this study.

The phylogenetic tree was performed using the MEGA 11.0 and was displayed by ITOL (https://itol.embl.de/).

Multiple sequence alignments

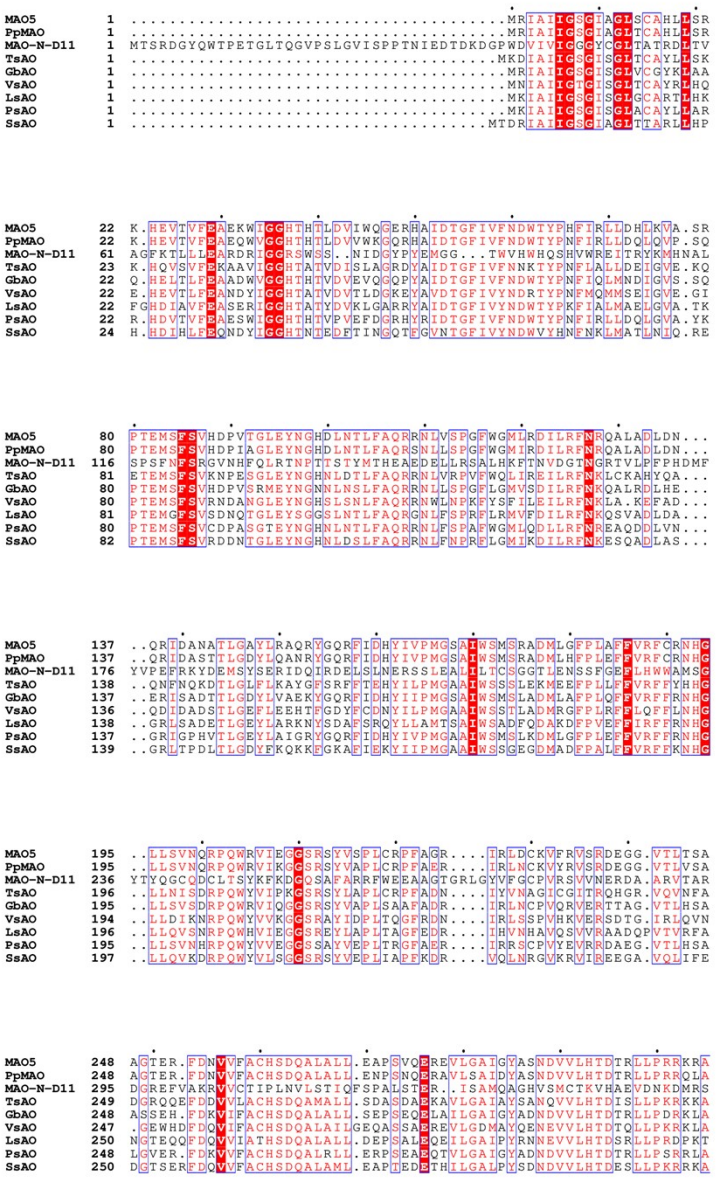

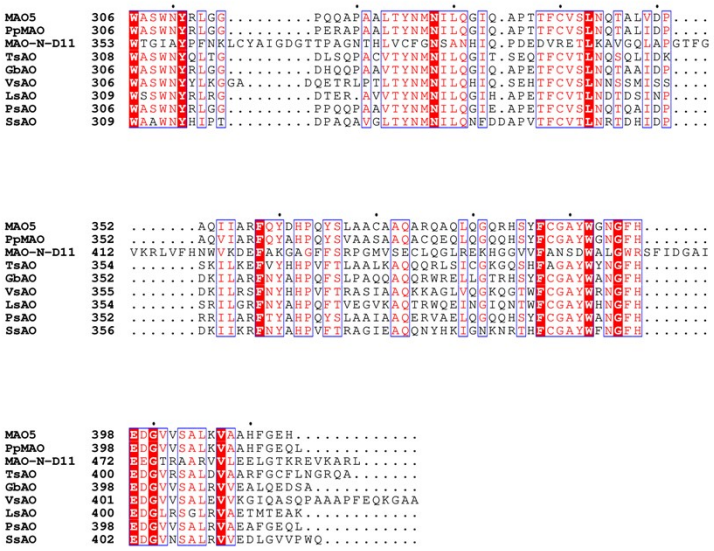

Figure S2. Multiple sequence alignments of these AOs used in this study.

Corresponding sources and GenBank accession numbers were given in Table S1. Multiple sequence alignments were performed using the MEGA server (https://www.megasoftware.net/show_eua) and displayed using ESPript (https://espript.ibcp.fr/ESPript/ESPript/index.php).

SDS-PAGE analysis

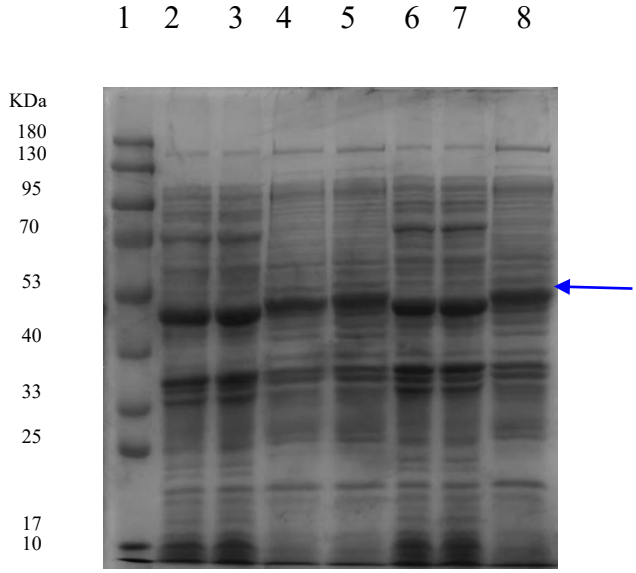

Figure S3. SDS-PAGE analysis of expression level of AOs.

Lane 1, protein markers. Lane 2, crude extract of *Gb*AO. Lane 3, crude extract of *Ps*AO. Lane 4, crude extract of *Ss*AO. Lane 5, crude extract of *Ts*AO. Lane 6, crude extract of MAO5. Lane 7, crude extract of *Ls*AO. Lane 8, crude extract of *Vs*AO. Seven proteins are soluble which have similar molecular mass of approximately 50 KDa.

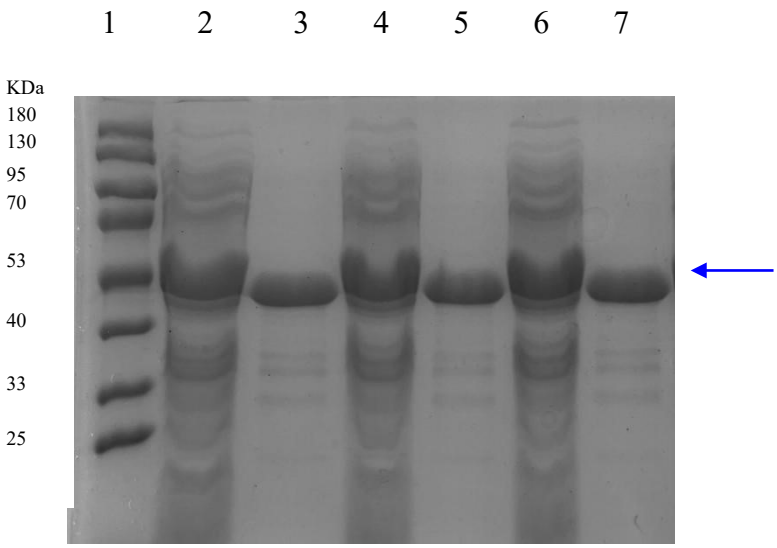

Figure S4. SDS-PAGE analysis of expression level of *Vs*AO and its mutant**.**

Lane 1, protein markers. Lane 2, crude extract of *Vs*AO. Lane 3, purified *Vs*AO. Lane 4, crude extract of M1. Lane 5, purified M1. Lane 6, crude extract of M2. Lane 7, purified M2. Four proteins are soluble which have the same molecular mass of approximately 50 KDa.

Enzymatic properties of *Vs*AO

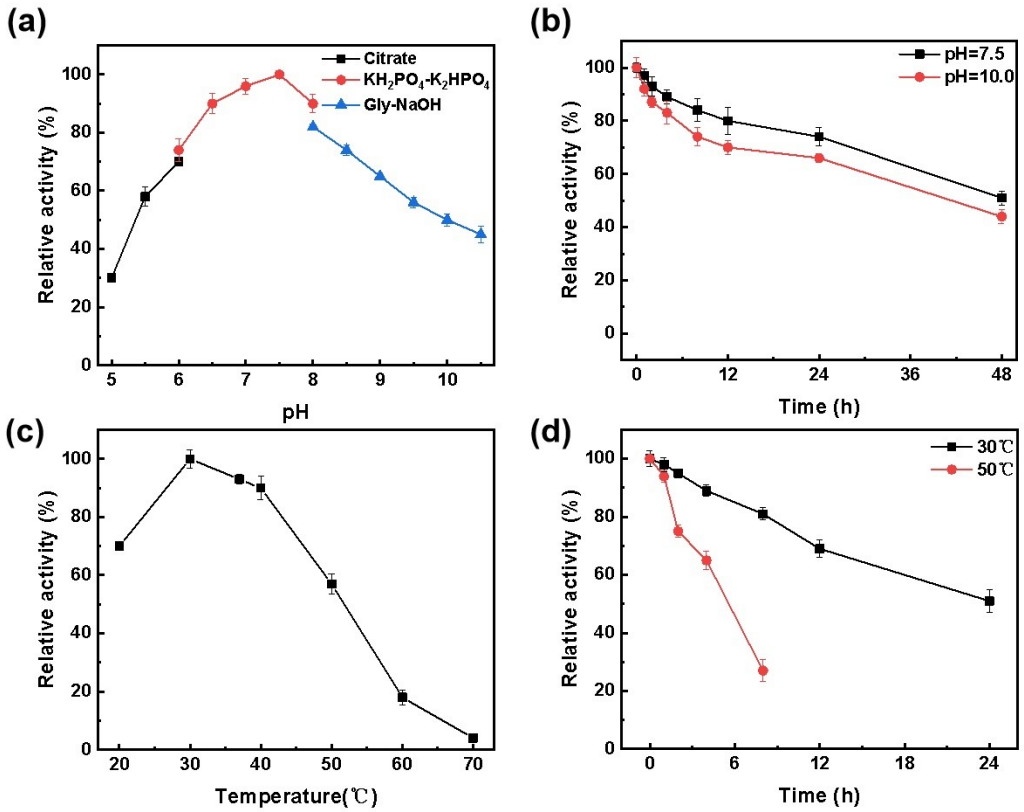

Figure S5. Effect of temperature and pH on the enzyme activity and stability of *Vs*AO. (a) Effect of pH on the enzyme activity was determined by measuring the activity at various buffers (pH 5.0-10.5) at 37°C. The value at pH 7.5 was taken as 100%. (b) Effect of pH on the enzyme stability was evaluated by measuring the residual activity after incubation of the enzyme in different buffers (pH 7.5, 10.0) at 25°C. (c) Effect of temperature on the enzyme activity was determined by measuring the activity at various temperatures (20-70°C) at pH 7.5. The value at 30°C was set as 100%. (d) Effect of temperature on the enzyme stability was determined by measuring the remaining activity after incubation of the enzyme at 30 and 50°C. All experiments were performed in triplicate. Each data point represents the mean ± the standard deviation of three measurements.

Mutagenesis

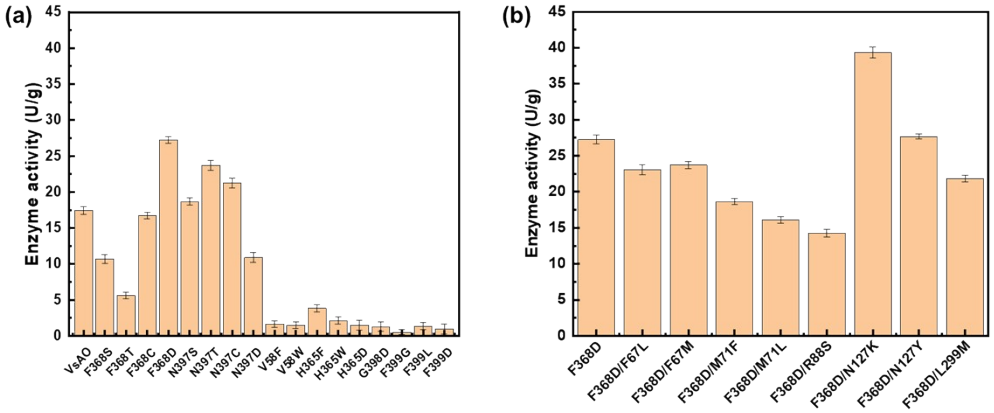

Figure S6. (a) first round of mutation screening. (b) second round of mutation screening.

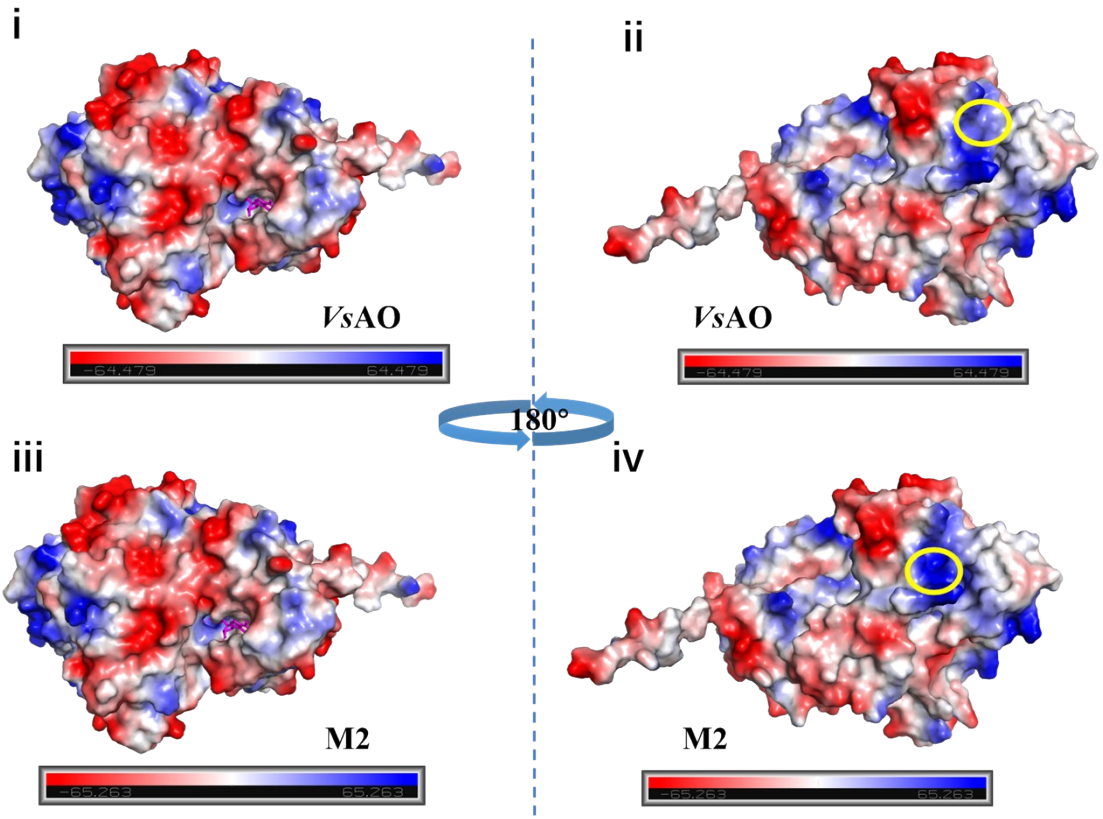

Figure S7. Surface potential simulation of (i, ii) *Vs*AO and (iii, iv) M2.

Enzymatic properties of M2

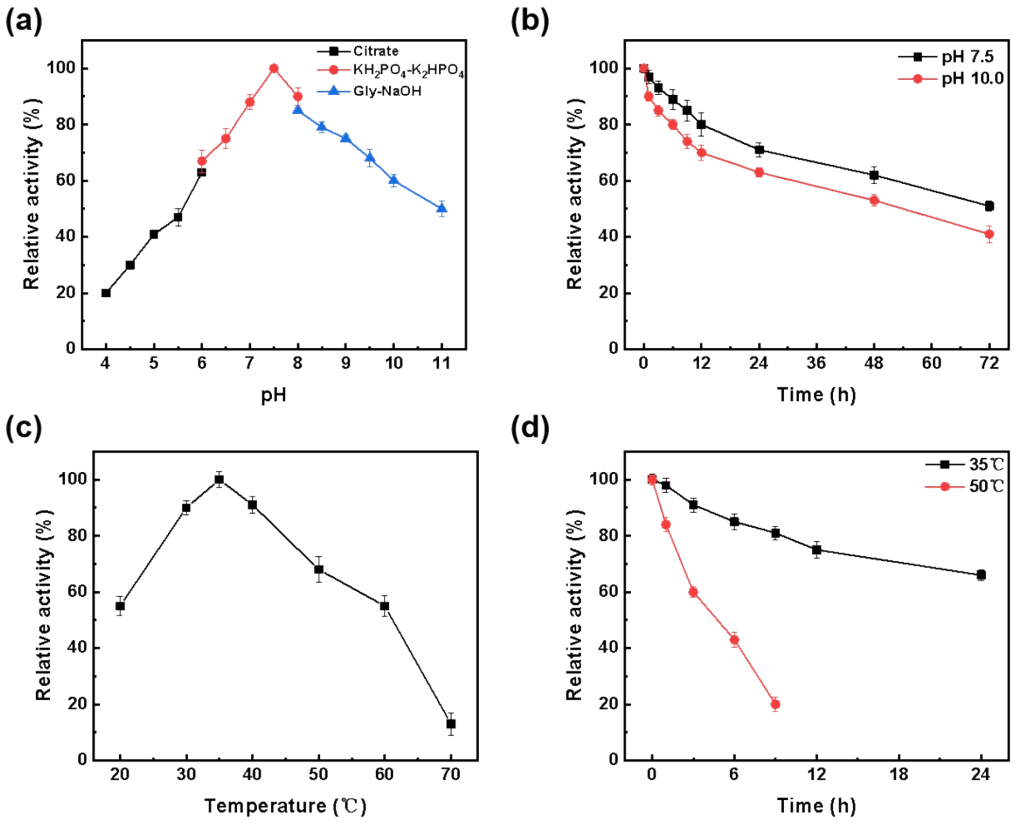

Figure S8. Effect of temperature and pH on the enzyme activity and stability of M2.

(a) Effect of pH on the enzyme activity was determined by measuring the activity at various buffers (pH 4.0-11.0) at 30°C. The value at pH 7.5 was taken as 100%. (b) Effect of pH on the enzyme stability was evaluated by measuring the residual activity after incubation of the enzyme in different buffers (pH 7.5, 10.0) at 25°C. (c) Effect of temperature on the enzyme activity was determined by measuring the activity at various temperatures (20-70°C) at pH 7.5. The value at 35°C was set as 100%. (d) Effect of temperature on the enzyme stability was determined by measuring the remaining activity after incubation of the enzyme at 35 and 50°C. All experiments were performed in triplicate. Each data point represents the mean ± the standard deviation of three measurements.

Kinetic parameters

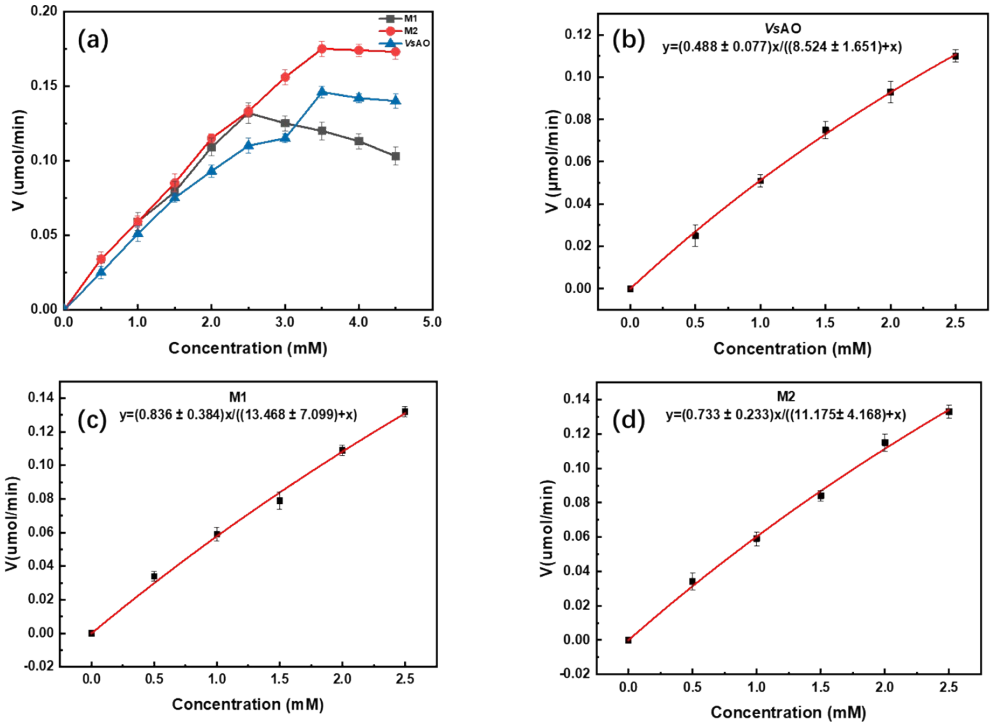

Figure S9. Kinetic parameters for the oxidative dehydroaromatization of substrate **1a** by *Vs*AO and its mutants**.**

(a) Effect of substrate concentration on the oxidative dehydroaromatization reaction initial rate. (b) Kinetic parameters for the oxidative dehydroaromatization of substrate **1a** by *Vs*AO. (c) Kinetic parameters for the oxidative dehydroaromatization of substrate **1a** by M1. (d) Kinetic parameters for the oxidative dehydroaromatization of substrate **1a** by M2. All experiments were performed in triplicate. Each data point represents the mean ± the standard deviation of three measurements.

Table S1. List of protein information of enzymes used in this study.

Enzyme	Source	GenBank Accession Number	Protein sequence identity（%）
*Gb*AO	*Gammaproteobacteria bacterium*	MCL5043555.1	72
*Ps*AO	*Pseudomonas* sp.	HCW97116.1	75
*Ss*AO	*Saccharospirillum* sp.	MCH8530221.1	55
*Ts*AO	*Thalassomonas* sp. RHCI1	WP_281556337.1	57
*Ls*AO	*Luminiphilus* sp.	MDB4491165.1	57
*Vs*AO	*Vibrio* sp. JCM 19236	GAM70821.1	55
MAO5	*Pseudomonas monteilii* ZMU-T01	WP_013972159.1	100

Table S2. Amino acid sequence of MAO5[2]

AMINO ACID SEQUENCE OF MAO5
MRIAIIGSGIAGLSCAHLLSRKHEVTVFEAEKWIGGHTHTLDVIWQGERHAI
DTGFIVFNDWTYPHFIRLLDHLKVASRPTEMSFSVHDPVTGLEYNGHDLNT
LFAQRRNLVSPGFWGMLRDILRFNRQALADLDNQRIDANATLGAYLRAQR
YGQRFIDHYIVPMGSAIWSMSRADMLGFPLAFFVRFCRNHGLLSVNQRPQ
WRVIEGGSRSYVSPLCRPFAGRIRLDCKVFRVSRDEGGVTLTSAAGTERFD
NVVFACHSDQALALLEAPSVQEREVLGAIGYASNDVVLHTDTRLLPRRKR
AWASWNYRLGGPQQAPAALTYNMNILQGIQAPTTFCVSLNQTALVDPAQII
ARFQYDHPQYSLAACAAQARQAQLQGQRHSYFCGAYWGNGFHEDGVVS
ALKVAAHFGEHL

Table S3. The physical and chemical properties of candidates predicted by Expasy and Protein-Sol.

Enzyme	Predicted solubility	Theoretical pI	Instability index	Estimated half-life (hour)
*Vs*AO	0.243	5.51	36.52	>10
*Ls*AO	0.103	6.02	37.39	>10
*Ts*AO	0.139	8.46	39.86	>10
*Ss*AO	0.212	6.01	40.72	>10
*Ps*AO	0.124	6.20	45.51	>10
*Gb*AO	0.123	5.64	37.14	>10
MAO5	0.083	8.91	35.34	>10

Table S4. Screening for the forms of biocatalyst [a,b,c].

Catalyst form	Conversion[b] (%)	Yield[c] (%)
Crude extract	60	48
Wet whole cells	67	56
Freeze-dried whole cells	68	58

[a]*Reaction conditions* (5.0 mL): **1a** (5.0 mM) and catalyst in KH_2PO_4-K_2HPO_4 buffer (pH 7.5, 50 mM), and incubated at 37℃ and shaken at 200 rpm for 24 h. [b]The conversion was determined by HPLC. Conversion = $[n(mol)_{initial\ substrate} - n(mol)_{residual\ substrate}/n(mol)_{initial\ substrate}] \times 100\%$. [c]The yield was determined by HPLC. Yield = $[n(mol)_{generated\ product}/n(mol)_{initial\ substrate}] \times 100\%$.

Table S5. Optimization of reaction conditions for oxidative dehydroaromatization of substrate 1a by *Vs*AO[a,b,c,d,e].

Entry	Buffer (50 mM)	Temperature (℃)	Concentration of biocatalyst (g/L)	Conversion[b] (%)	Yield[c] (%)
1	KH_2PO_4-K_2HPO_4 (pH 7.0)	37	8	60	48
2	KH_2PO_4-K_2HPO_4 (pH 7.5)	37	8	67	55
3	KH_2PO_4-K_2HPO_4 (pH 8.0)	37	8	59	45
4	Gly-NaOH (pH 8.0)	37	8	51	40
5	Gly-NaOH (pH 8.5)	37	8	48	38
6	Gly-NaOH (pH 9.0)	37	8	46	35
7	KH_2PO_4-K_2HPO_4 (pH 7.5)	20	8	62	53
8	KH_2PO_4-K_2HPO_4 (pH 7.5)	25	8	69	56
9	KH_2PO_4-K_2HPO_4 (pH 7.5)	30	8	71	60
10	KH_2PO_4-K_2HPO_4 (pH 7.5)	37	8	67	55
11	KH_2PO_4-K_2HPO_4 (pH 7.5)	40	8	58	44
12	KH_2PO_4-K_2HPO_4 (pH 7.5)	30	4	60	48
13	KH_2PO_4-K_2HPO_4 (pH 7.5)	30	8	71	60
14	KH_2PO_4-K_2HPO_4 (pH 7.5)	30	12	83	70
15	KH_2PO_4-K_2HPO_4 (pH 7.5)	30	16	91	76
16	KH_2PO_4-K_2HPO_4 (pH 7.5)	30	20	79	72
17	KH_2PO_4-K_2HPO_4 (pH 7.5)	30	30	69	62
18	KH_2PO_4-K_2HPO_4 (pH 7.5)	30	40	67	56
19[d]	KH_2PO_4-K_2HPO_4 (pH 7.5)	30	16	92	78
20[e]	KH_2PO_4-K_2HPO_4 (pH 7.5)	30	16	99	83

[a]*Reaction conditions* (5.0 mL): **1a** (5 mM) and lyophilized whole cells in KH_2PO_4-K_2HPO_4 or Gly-NaOH buffer (50 mM). Reactions were incubated at 30℃ and shaken at 200 rpm for 24 h. [b]The conversion was determined by HPLC. Conversion = $[n(mol)_{initial\ substrate} - n(mol)_{residual\ substrate}/n(mol)_{initial\ substrate}] \times 100\%$. [c]The yield was

determined by HPLC. Yield = [$n(mol)_{generated\ product}/n(mol)_{initial\ substrate}$] × 100%. [d]Catalase was added. [e] Reaction was extended to 48 h.

Table S6. Gene sequence of wild-type *Vs*AO

GENE SEQUENCE OF WILD-TYPE *Vs*AO
ATGAACATCGCGATCATCGGTACCGGTATCAGCGGCCTGACCTGCGCGT
ACCGTCTGCACCAGGAACACGAAGTTACCCTGTTCGAAGCGAACGACTA
CATCGGCGGTCATACCGCGACCGTTGATGTGACCCTGGATGGTAAAGAA
TACGCGGTTGACACCGGTTTCATCGTTTACAACGACCGCACCTACCCGA
ACTTCATGCAGATGATGTCTGAAATCGGCGTTGAAGGTATCCCGACCGA
AATGAGCTTCTCTGTTCGCAACGATGCGAACGGCCTGGAATACAACGGC
CACTCCCTGTCTAACCTGTTCGCGCAGAAACGTAACTGGCTGAACCCGA
AATTCTACTCCTTCATCCTGGAAATCCTGCGTTTTAACAAACTGGCGAA
AGAATTCGCGGATCAGGATATCGATGCGGATAGCACCCTGGGTGAATTC
CTGGAAGAACACACTTTCGGCGATTACTTTTGCGATAACTACATCCTGC
CGATGGGCGCGGCGATTTGGTCCTCTACCCTGGCGGATATGCGTGGCTT
CCCGCTGCGTTTCTTCCTGCAGTTCTTCCTGAACCACGGCCTGCTGGATA
TCAAAAACCGTCCGCAGTGGTACGTTGTTAAAGGTGGTAGCCGTGCGTA
TATCGATCCGCTGACCCAGGGTTTCCGTGATAACATTCGTCTGAGCTCCC
CGGTTCACAAAGTTGAACGTTCCGATACCGGCATCCGTCTGCAGGTGAA
CGGCGAATGGCACGATTTCGATCAGGTGATTTTCGCCTGCCACAGCGAT
CAGGCGCTGGCTATCCTGGGCGAACAGGCGAGCTCCGCGGAACGTGAA
GTTCTGGGCGATATGGCGTACCAGGAAAACGAAGTTGTTCTGCATACCG
ATACCCAGCTGCTGCCGAAACGTAAACTGGCCTGGGCGAGCTGGAACT
ATTACCTGAAAGGCGGCGCGGACCAGGAAACCCGTCTGCCGACCCTGA
CCTACAACATGAACATCCTGCAGCACATCCAGTCTGAACACACCTTCTG
TGTTTCTCTGAACAACAGCTCTATGATCTCTTCTGATAAAATCCTGCGTT
CTTTCAACTACCACCACCCGGTTTTCACCCGTGCTAGTATCGCGGCGCA
GAAAAAAGCTGGCCTGGTTCAGGGCAAACAGGGTACCTGGTTCTGCGG
CGCGTACTGGCGTAACGGTTTTCACGAAGATGGTGTTGTTAGCGCACTG
GAAGTTGTTAAAGGTATCCAGGCTTCTCAGCCGGCAGCTGCGCCGTTCG
AACAGAAAGGCGCGGCGCTCGAG

Table S7. Primers used for site-directed mutagenesis.

PRIMER	SEQUENCE (5’ TO 3’)
V58F-FP	CGGTTTCATCTTTTACAACGACCGC
V58F-RP	GGTCGTTGTAAAAGATGAAACCGGTG
V58W-FP	CGGTTTCATCTGGTACAACGACC
V58W-RP	GTCGTTGTACCAGATGAAACCGG
N127R-FP	TCCTGCGTTTTAGAAAACTGGCGA
N127R-RP	TTCGCCAGTTTTCTAAAACGCAGGAT
N127W-FP	TCCTGCGTTTTTGGAAACTGGC
N127W-RP	CCAGTTTCCAAAAACGCAGGATT
H365F-FP	TCAACTACCACTTTCCGGTTTTCACC
H365F-RP	GGTGAAAACCGGAAAGTGGTAGTTG
H365W-FP	CAACTACCACTGGCCGGTTTTC
H365W-RP	AAAACCGGCCAGTGGTAGTTGA
H365D-FP	CAACTACCACGATCCGGTTTTCAC
H365D-RP	TGAAAACCGGATCGTGGTAGTTGAA
G398D-FP	CTGGCGTAACGATTTTCACGAAGAT
G398D-RP	CTTCGTGAAAATCGTTACGCCAGT
F399G-FP	GTAACGGTGGACACGAAGATGG
F399G-RP	ACCATCTTCGTGTCCACCGTTA
F399L-FP	CGTAACGGTCTTCACGAAGATGG
F399L-RP	CATCTTCGTGAAGACCGTTACGC
F399D-FP	CGTAACGGTGATCACGAAGATGG
F399D-RP	CATCTTCGTGATCACCGTTACGC
N127K-FP	AAATCCTGCGTTTTAAGAAACTGGCGAAAG A
N127K-RP	ATTCTTTCGCCAGTTTCTTAAAACGCAGGAT

N127Y-FP	AAATCCTGCGTTTTTATAAACTGGCGAAAGA
N127Y-RP	AATTCTTTCGCCAGTTTATAAAAACGCAGGA T
L299M-FP	GATACCCAGCTGATGCCGAAACGTAAA
L299M-RP	AGTTTACGTTTCGGCATCAGCTGGGTA
F67L-FP	ACCTACCCGAACCTTATGCAGATGATGT
F67L-RP	CATCATCTGCATAAGGTTCGGGTAGGTG
F67M-FP	ACCTACCCGAACATGATGCAGATGATGT
F67M-RP	ATCATCTGCATCATGTTCGGGTAGGTGC
R88S-FP	GAGCTTCTCTGTTTCTAACGATGCGAACGG
R88S-RP	CGTTCGCATCGTTAGAAACAGAGAAGCTCA
M71F-FP	CTTCATGCAGATGTTTTCTGAAATCGGCGT
M71F-RP	AACGCCGATTTCAGAAAACATCTGCATGAA
M71L-FP	ACTTCATGCAGATGCTTTCTGAAATCGGCGT
M71L-RP	AACGCCGATTTCAGAAAGCATCTGCATGAA G
F368S-FP	ACCCGGTTTCTACCCGTGCTAGTAT
F368S-RP	TAGCACGGGTAGAAACCGGGT
F368T-FP	CACCCGGTTACCACCCGTGCTAGTATC
F368T-RP	ATACTAGCACGGGTGGTAACCGGGT
F368C-FP	ACCCGGTTTGCACCCGTGCTAGTAT
F368C-RP	GATACTAGCACGGGTGCAAACCGGGT
F368D-FP	ACCCGGTTGATACCCGTGCTA
F368D-RP	ATACTAGCACGGGTATCAACCGGG
N397S-FP	TACTGGCGTTCCGGTTTTCACG
N397S-RP	TGAAAACCGGAACGCCAGTACG
N397T-FP	TACTGGCGTACCGGTTTTCACGA
N397T-RP	TGAAAACCGGTACGCCAGTACG

N397C-FP	TACTGGCGTTGCGGTTTTCACG
N397C-RP	AAAACCGCAACGCCAGTACG
N397D-FP	TACTGGCGTGATGGTTTTCACG
N397D-RP	AAAACCATCACGCCAGTACGC

Table S8. Kinetic parameters for the oxidative dehydroaromatization of substrate 1a by *Vs*AO and its mutants.[a,b]

Enzyme	V_{max}	k_{cat} (min^{-1})	K_M (mM)	k_{cat}/K_M ($min^{-1}mM^{-1}$)	Activity[b] (U/g)
*Vs*AO	0.488	7.9	8.5	0.9	17.4
M1(F368D)	0.836	14.5	13.5	1.1	27.2
M2 (F368D/N127K)	0.733	13.7	11.2	1.2	40.3

[a]Kinetic parameters were determined in potassium phosphate buffer (50 mM, pH 7.5) containing purified AOs and varied concentration of 1a at 30℃. [b]The activity assay was carried out in 1 mL reaction mixture containing potassium phosphate buffer (50 mM, pH 7.5), substrate **1a** (5 mM) and appropriate purified enzyme solution at 30℃.

Table S9. Comparison between classical chemical catalytic method and biocatalytic method for the oxidative dehydroaromatization of THQ.

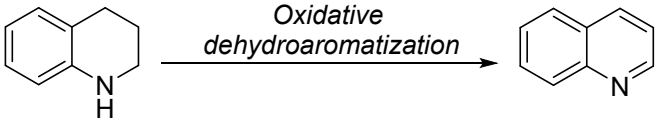

Catalyst	Reaction condition	Yield	Reference
$NiBr_2$	*t*-amyl alcohol, TEMPO, *t*-BuOK, 95℃, 24 h, 250 mM, 0.025 mmol catalyst, 0.1 MPa O_2	99%	[3]
Co-Phen@C	n-decane, *t*-BuOK, 150℃, 36 h, 250 mM, 0.03 mmol catalyst, 0.1 MPa Ar.	93%	[4]
NPCH	H_2O, 0.1 MPa air, 120℃, 12 h, 133 mM, 5 mg catalyst	94%	[5]
Co/MC	acetonitrile, 2.5 bar O_2, 150℃, 12 h, 100 mM, 20 mg catalyst	97.6%	[6]
Acceptorless method	*o*-xylene, *t*-BuOK, 140℃, 36 h, 250 mM, 0.1 MPa N_2	92%	[7]
M2 (mutant of *Vs*AO)	KPi buffer, air, 30℃, 12 h, 5 mM, 16 g/L lyophilized whole cells	88%	This work

Table S10. Optimization of the type and content of co-solvents for oxidative dehydroaromatization of substrate 5a by *Vs*AO[a,b].

Entry	Type and Content of Co-solvent(v/v)	Yield[b]（%）
1	PBS buffer	64
2	10% DMSO	73
3	10% Dodecane	54
4	10% Ethanol	51
5	10% Isooctane	40
6	10% DMF	61
7	10% Oleic acid	15
8	10% 2-MeTHF	13
9	10% EtOAc	24
10	10% MTBE	37
11	5% DMSO	70
12	10% DMSO	73
13	15% DMSO	71
14	20% DMSO	69

[a]*Reaction conditions* (5.0 mL): **5a** (10 mM), various co-solvent, freeze-dried whole cells (16 g/L), 5.0 mL KH_2PO_4-K_2HPO_4 buffer (pH 7.5, 50 mM). Reactions were incubated at 30°C and shaken at 200 rpm for 24 h. [b]The yield was determined by HPLC. Yield = $[n(mol)_{generated\ product}/n(mol)_{initial\ substrate}] \times 100\%$.

Characterization and NMR of products

^{1}H and ^{13}C NMR spectra of the products recorded in $CDCl_3$ or DMSO-d_6

2-Methylquinoline **1b**

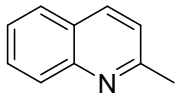

1b

^{1}H NMR (400 MHz, Chloroform-*d*) δ 8.03 (d, *J* = 8.3 Hz, 2H), 7.76 (d, *J* = 8.1 Hz, 1H), 7.68 (t, *J* = 7.7 Hz, 1H), 7.47 (t, *J* = 7.6 Hz, 1H), 7.28 (s, 1H), 2.75 (s, 3H).**^{13}C NMR** (151 MHz, Chloroform-*d*) δ 159.05, 147.98, 136.23, 129.49, 128.73, 127.56, 126.58, 125.74, 122.05, 25.44.

6-Fluoro-2-Methylquinoline **2b**

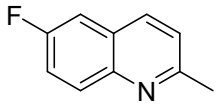

2b

^{1}H NMR (400 MHz, Chloroform-*d*) δ 8.02 – 7.90 (m, 2H), 7.41 (td, *J* = 8.8, 2.7 Hz, 1H), 7.37 – 7.30 (m, 1H), 7.24 (s, 1H), 2.69 (s, 3H).**^{13}C NMR** (151 MHz, Chloroform-*d*) δ 160.12 (d, *J* = 246.8 Hz), 158.40 (d, *J* = 2.7 Hz), 145.01, 135.70 (d, *J* = 5.1 Hz), 131.11 (d, *J* = 9.1 Hz), 127.12 (d, *J* = 9.8 Hz), 122.88, 119.62 (d, *J* = 25.6 Hz), 110.64 (d, *J* = 21.4 Hz), 25.29.

6-Bromo-2-Methylquinoline **3b**

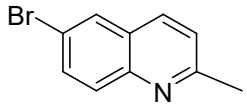

3b

^{1}H NMR (400 MHz, Chloroform-*d*) δ 7.92 – 7.82 (m, 3H), 7.70 (dd, *J* = 8.9, 2.2 Hz, 1H), 7.24 (s, 1H), 2.70 (s, 3H).**^{13}C NMR** (151 MHz, Chloroform-*d*) δ 159.63, 146.54, 135.30, 132.98, 130.52, 129.65, 127.77, 122.97, 119.54, 25.46.

Quinoline **4b**

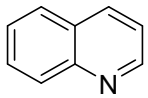

4b

^{1}H NMR (400 MHz, Chloroform-*d*) δ 8.91 (d, *J* = 4.3 Hz, 1H), 8.12 (t, *J* = 9.0 Hz, 2H), 7.80 (d, *J* = 8.2 Hz, 1H), 7.70 (t, *J* = 7.7 Hz, 1H), 7.53 (t, *J* = 7.6 Hz, 1H), 7.37 (dd, *J* = 8.4, 4.2 Hz, 1H).**^{13}C NMR** (151 MHz, Chloroform-*d*) δ 150.44, 148.38, 136.05, 129.54, 129.48, 128.35, 127.83, 126.57, 121.10.

6-Fluoroquinoline **5b**

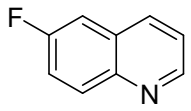

5b

^{1}H NMR (400 MHz, Chloroform-*d*) δ 8.73 (d, *J* = 4.2 Hz, 1H), 7.96 (dd, *J* = 9.2, 6.6 Hz, 2H), 7.33 (td, *J* = 8.8, 2.7 Hz, 1H), 7.30 – 7.21 (m, 2H).**^{13}C NMR** (151 MHz, Chloroform-*d*) δ 160.44 (d, *J* = 248.4 Hz), 149.67 (d, *J* = 2.7 Hz), 145.39, 135.47 (d, *J* = 5.4 Hz), 131.98 (d, *J* = 9.2 Hz), 128.94 (d, *J* = 10.2 Hz), 121.80, 119.79 (d, *J* = 26.0 Hz), 110.73 (d, *J* = 21.4 Hz).

6-Bromoquinoline **6b**

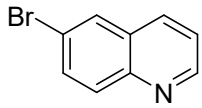

6b

^{1}H NMR (400 MHz, Chloroform-*d*) δ 8.89 (d, *J* = 4.2 Hz, 1H), 8.03 (d, *J* = 8.3 Hz, 1H), 7.95 (d, *J* = 8.8 Hz, 2H), 7.75 (dd, *J* = 9.0, 2.1 Hz, 1H), 7.39 (dd, *J* = 8.4, 4.2 Hz, 1H).**^{13}C NMR** (151 MHz, Chloroform-*d*) δ 150.63, 146.74, 134.91, 132.84, 131.15, 129.71, 129.24, 121.79, 120.39.

6-Chloroquinoline **7b**

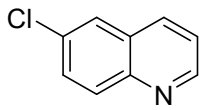

7b

^{1}H NMR (400 MHz, Chloroform-*d*) δ 8.78 (d, *J* = 4.2 Hz, 1H), 7.92 (dd, *J* = 8.7, 4.7 Hz, 2H), 7.64 (d, *J* = 2.4 Hz, 1H), 7.52 (dd, *J* = 8.9, 2.4 Hz, 1H), 7.32 – 7.23 (m, 1H).**^{13}C NMR** (151 MHz, Chloroform-*d*) δ 150.65, 146.73, 135.23, 132.43, 131.21, 130.53, 128.95, 126.51, 122.00.

6-Phenylquinoline **8b**

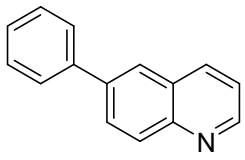

8b

^{1}H NMR (600 MHz, Chloroform-*d*) δ 8.14 (s, 1H), 7.94 (s, 1H), 7.67 (s, 1H), 7.53 (s, 1H), 7.44 (s, 1H), 7.37 (s, 2H), 7.31 (s, 2H), 7.09 (s, 1H), 6.93 (s, 1H).**^{13}C NMR** ^{13}C NMR (151 MHz, Chloroform-*d*) δ 150.21, 147.39, 145.83, 136.13, 132.18, 131.42, 129.69, 128.84, 127.63, 127.44, 127.27, 125.96, 125.33, 121.38, 120.10.

6-Methoxyquinoline **9b**

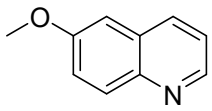

9b

^{1}H NMR (400 MHz, Chloroform-*d*) δ 8.74 (dd, *J* = 4.0, 1.7 Hz, 1H), 8.00 (dd, *J* = 10.6, 8.9 Hz, 2H), 7.33 (ddd, *J* = 14.1, 8.6, 3.4 Hz, 2H), 7.03 (d, *J* = 2.8 Hz, 1H), 3.89 (d, *J* = 1.4 Hz, 3H).**^{13}C NMR** (151 MHz, Chloroform-*d*) δ 157.63, 147.79, 144.35, 134.64, 130.72, 129.22, 122.15, 121.23, 105.07, 55.38.

6-Hydroxyquinoline **10b**

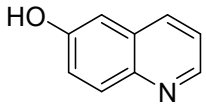

10b

^{1}H NMR (400 MHz, DMSO-d_6) δ 9.19 (s, 1H), 7.75 (d, *J* = 4.1 Hz, 1H), 7.22 (d, *J* = 8.3 Hz, 1H), 6.96 (d, *J* = 9.0 Hz, 1H), 6.52 – 6.39 (m, 2H), 6.26 (d, *J* = 2.6 Hz, 1H).**^{13}C NMR** (151 MHz, DMSO-d_6) δ 155.43, 147.02, 143.01, 134.03, 130.31, 129.25, 121.91, 121.31, 108.29.

3-Methylquinoline **11b**

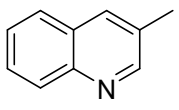

11b

^{1}H NMR (400 MHz, Chloroform-*d*) δ 8.75 (d, *J* = 2.3 Hz, 1H), 8.06 (d, *J* = 8.4 Hz, 1H), 7.88 (s, 1H), 7.71 (d, *J* = 8.2 Hz, 1H), 7.67 – 7.58 (m, 1H), 7.53 – 7.44 (m, 1H),

2.49 (s, 3H).**^{13}C NMR** (151 MHz, Chloroform-*d*) δ 152.37, 146.57, 134.69, 130.47, 129.17, 128.46, 128.17, 127.15, 126.56, 18.73.

4-Methylquinoline **12b**

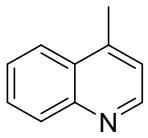

12b

^{1}H NMR (400 MHz, Chloroform-*d*) δ 8.82 (d, *J* = 4.3 Hz, 1H), 8.17 (d, *J* = 8.5 Hz, 1H), 8.03 (d, *J* = 8.4 Hz, 1H), 7.76 (t, *J* = 7.7 Hz, 1H), 7.61 (t, *J* = 7.7 Hz, 1H), 7.27 (s, 1H), 2.74 (s, 3H).**^{13}C NMR** (151 MHz, Chloroform-*d*) δ 150.16, 148.03, 144.25, 130.05, 129.09, 128.30, 126.28, 123.81, 121.85, 18.61.

5-Methylquinoline **13b**

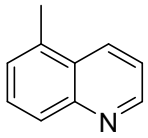

13b

^{1}H NMR (600 MHz, Chloroform-*d*) δ 8.89 (dd, *J* = 4.1, 1.6 Hz, 1H), 8.29 (dd, *J* = 8.5, 1.5 Hz, 1H), 7.96 (d, *J* = 8.4 Hz, 1H), 7.58 (dd, *J* = 8.4, 7.0 Hz, 1H), 7.38 (dd, *J* = 8.5, 4.1 Hz, 1H), 7.34 (d, *J* = 7.0 Hz, 1H), 2.65 (s, 3H).**^{13}C NMR** (151 MHz, Chloroform-d) δ 149.77, 148.47, 134.44, 132.28, 129.00, 127.64, 127.50, 126.87, 120.52, 18.38.

6-Methylquinoline **14b**

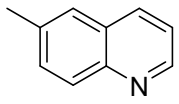

14b

^{1}H NMR (400 MHz, Chloroform-*d*) δ 8.83 (d, *J* = 4.2 Hz, 1H), 8.01 (dd, *J* = 16.9, 8.4 Hz, 2H), 7.57 – 7.49 (m, 2H), 7.33 (dd, *J* = 8.3, 4.2 Hz, 1H), 2.52 (s, 3H).**^{13}C NMR** (151 MHz, Chloroform-*d*) δ 149.44, 146.89, 136.28, 135.25, 131.65, 129.07, 128.27, 126.53, 120.98, 21.48.

7-Methylquinoline **15b**

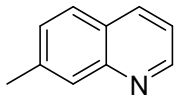

15b

^{1}H NMR (600 MHz, Chloroform-*d*) δ 8.85 (dd, *J* = 4.0, 1.8 Hz, 1H), 8.07 (dd, *J* = 8.3, 1.7 Hz, 1H), 7.88 (s, 1H), 7.68 (d, *J* = 8.2 Hz, 1H), 7.35 (dd, *J* = 8.3, 1.7 Hz, 1H), 7.29 (ddd, *J* = 8.2, 4.3, 1.3 Hz, 1H), 2.55 (s, 3H).**^{13}C NMR** (151 MHz, Chloroform-*d*) δ 150.20, 148.43, 139.59, 135.55, 128.66, 128.31, 127.28, 126.24, 120.13, 21.72.

8-Methylquinoline **16b**

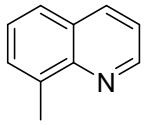

16b

^{1}H NMR (400 MHz, Chloroform-*d*) δ 8.98 – 8.92 (m, 1H), 8.13 (dd, *J* = 8.1, 1.8 Hz, 1H), 7.66 (d, *J* = 8.2 Hz, 1H), 7.56 (d, *J* = 7.0 Hz, 1H), 7.48 – 7.35 (m, 2H), 2.83 (s, 3H).**^{13}C NMR** (151 MHz, Chloroform-*d*) δ 149.29, 147.45, 137.16, 136.34, 129.68, 128.34, 126.35, 125.93, 120.87, 18.20.

7-Methoxyquinoline **17b**

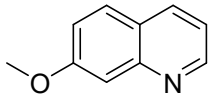

17b

^{1}H NMR (400 MHz, Chloroform-*d*) δ 8.80 (dd, *J* = 4.3, 1.9 Hz, 1H), 8.04 (d, *J* = 8.2 Hz, 1H), 7.66 (d, *J* = 9.0 Hz, 1H), 7.41 (d, *J* = 2.5 Hz, 1H), 7.21 (ddd, *J* = 21.5, 8.6, 3.4 Hz, 2H), 3.93 (s, 3H).**^{13}C NMR** (151 MHz, Chloroform-*d*) δ 160.71, 150.46, 149.91, 135.71, 128.79, 123.55, 119.81, 118.96, 107.28, 55.48.

7-Chloroquinoline **18b**

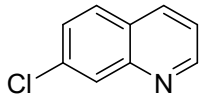

18b

^{1}H NMR (600 MHz, Chloroform-*d*) δ 8.78 (d, *J* = 4.4 Hz, 1H), 7.98 (q, *J* = 3.3, 2.9 Hz, 2H), 7.59 (d, *J* = 8.7 Hz, 1H), 7.35 (dd, *J* = 8.7, 2.1 Hz, 1H), 7.29 – 7.22 (m, 1H).**^{13}C**

NMR (151 MHz, Chloroform-*d*) δ 151.33, 148.57, 135.91, 135.33, 129.06, 128.45, 127.67, 126.65, 121.29.

7-Bromoquinoline **19b**

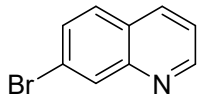

19b

^{1}H NMR (600 MHz, Chloroform-*d*) δ 8.91 (dt, *J* = 3.9, 1.8 Hz, 1H), 8.30 (d, *J* = 1.9 Hz, 1H), 8.12 (dd, *J* = 8.3, 1.8 Hz, 1H), 7.68 (dd, *J* = 8.6, 1.8 Hz, 1H), 7.63 (dt, *J* = 8.7, 2.0 Hz, 1H), 7.45 – 7.36 (m, 1H).**^{13}C NMR** (151 MHz, Chloroform-*d*) δ 151.38, 148.93, 136.12, 131.95, 130.31, 129.18, 127.02, 123.71, 121.53.

4-Hydroxyquinoline **20b**

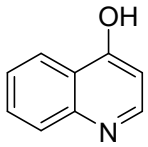

20b

^{1}H NMR (400 MHz, DMSO-d_6) δ 10.87 (s, 1H), 7.15 (d, *J* = 8.0 Hz, 1H), 6.95 (d, *J* = 7.2 Hz, 1H), 6.62 (dd, *J* = 30.0, 7.9 Hz, 2H), 6.34 (t, *J* = 7.5 Hz, 1H), 5.10 (d, *J* = 6.9 Hz, 1H).**^{13}C NMR** (151 MHz, DMSO-d_6) δ 176.87, 139.99, 139.31, 131.53, 125.79, 124.90, 122.98, 118.19, 108.65.

8-Hydroxyquinoline **21b**

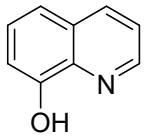

21b

^{1}H NMR (600 MHz, DMSO-d6) δ 9.84 (s, 1H), 8.83 (dd, J = 4.1, 1.7 Hz, 1H), 8.27 (dd, J = 8.3, 1.7 Hz, 1H), 7.50 (dd, J = 8.3, 4.1 Hz, 1H), 7.46 – 7.40 (m, 1H), 7.37 (dd, J = 8.2, 1.4 Hz, 1H), 7.12 (dd, J = 7.6, 1.4 Hz, 1H).**^{13}C NMR** (151 MHz, DMSO-d6) δ 153.26, 148.05, 138.47, 135.97, 128.74, 127.44, 121.74, 117.68, 111.21.

6-Bromo-4-Methylquinoline **22b**

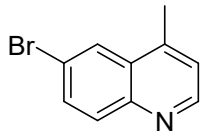

22b

^{1}H NMR (400 MHz, Chloroform-*d*) δ 8.77 – 8.71 (m, 1H), 8.10 (t, *J* = 1.7 Hz, 1H), 7.94 (dd, *J* = 9.0, 1.3 Hz, 1H), 7.73 (dt, *J* = 9.0, 1.8 Hz, 1H), 7.21 (d, *J* = 4.3 Hz, 1H), 2.63 (s, 3H).**^{13}C NMR** (151 MHz, Chloroform-*d*) δ 150.51, 146.61, 143.77, 132.77, 131.82, 129.67, 126.45, 122.70, 120.64, 18.75.

1-Methylisoquinoline **23b**

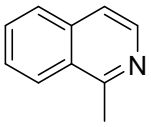

23b

^{1}H NMR (400 MHz, Chloroform-*d*) δ 8.37 (d, *J* = 5.8 Hz, 1H), 8.08 (d, *J* = 8.4 Hz, 1H), 7.77 (d, *J* = 8.2 Hz, 1H), 7.69 – 7.61 (m, 1H), 7.61 – 7.52 (m, 1H), 7.48 (d, *J* = 5.8 Hz, 1H), 2.95 (s, 3H).**^{13}C NMR** (151 MHz, Chloroform-*d*) δ 158.57, 141.77, 135.91, 129.92, 127.51, 127.19, 127.02, 125.60, 119.28, 22.36.

1-Phenylisoquinoline **24b**

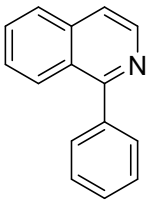

24b

^{1}H NMR (400 MHz, Chloroform-*d*) δ 8.62 (d, *J* = 5.6 Hz, 1H), 8.11 (d, *J* = 8.5 Hz, 1H), 7.88 (d, *J* = 8.2 Hz, 1H), 7.74 – 7.62 (m, 4H), 7.53 (dt, *J* = 10.1, 6.3 Hz, 4H). **^{13}C NMR** (151 MHz, Chloroform-*d*) δ 160.66, 142.08, 139.46, 136.82, 129.95, 129.85, 128.52, 128.26, 127.53, 127.10, 126.91, 126.66, 119.84

NMR spectra of products

2-Methylquinoline **1b**

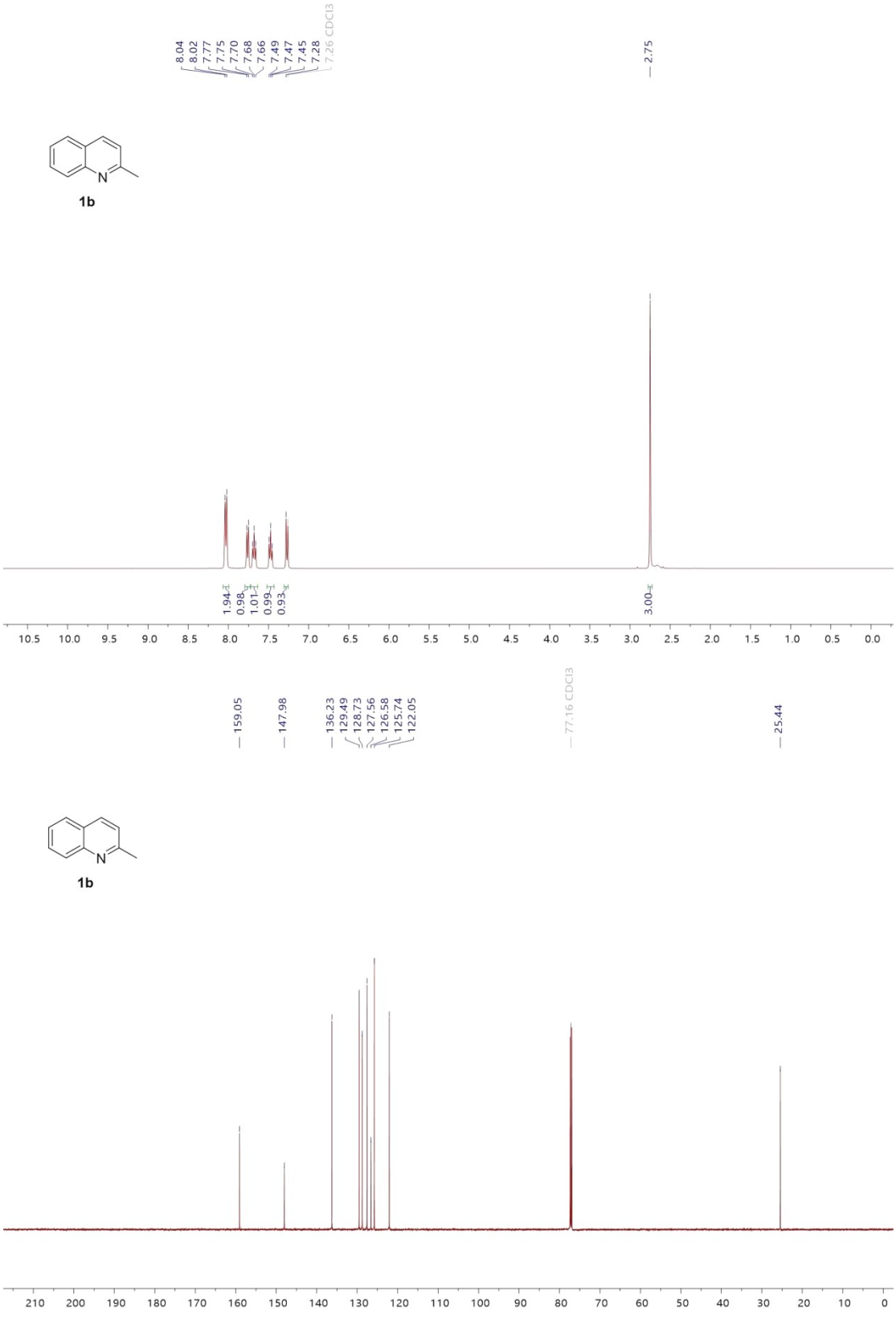

6-Fluoro-2-Methylquinoline **2b**

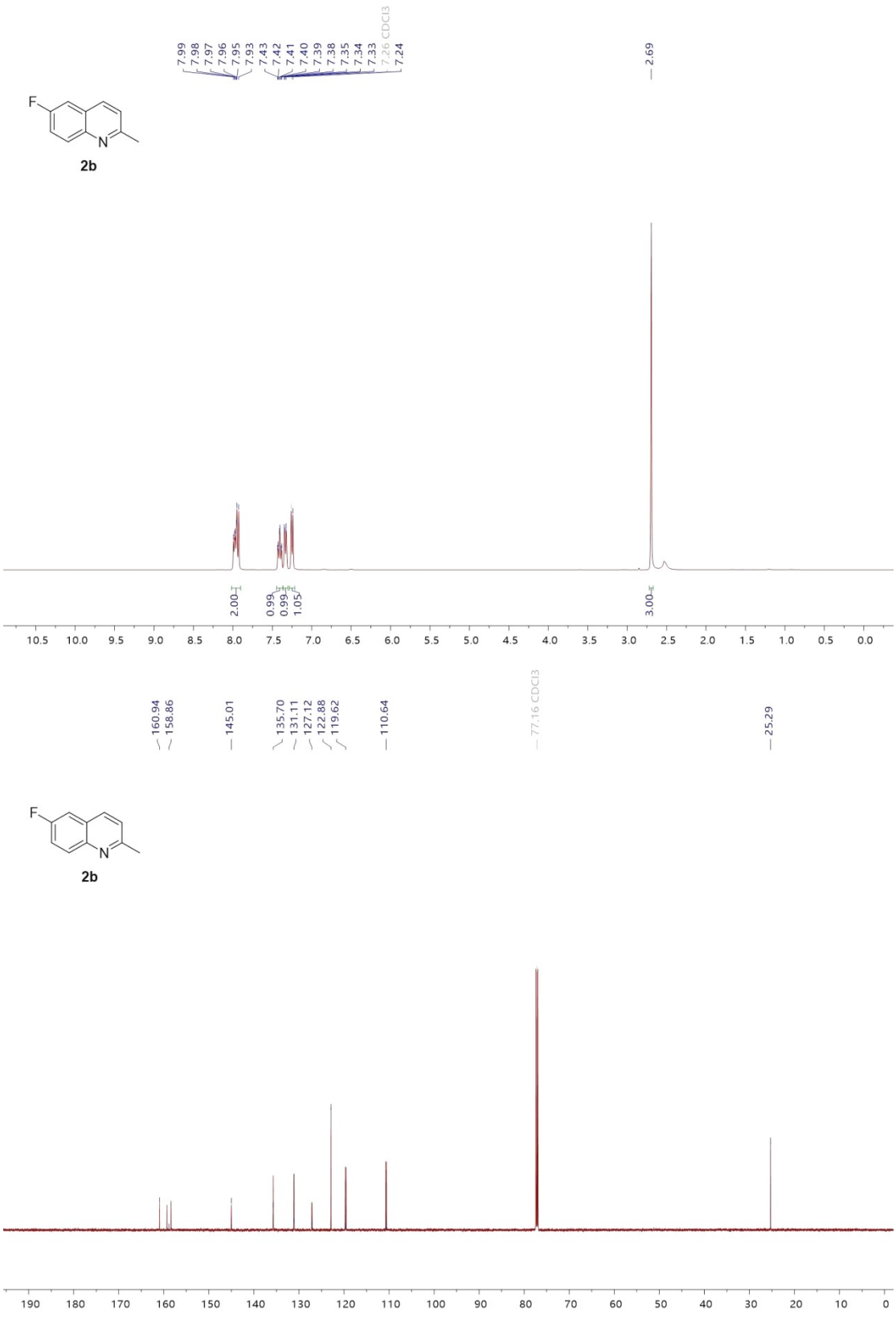

6-Bromo-2-Methylquinoline **3b**

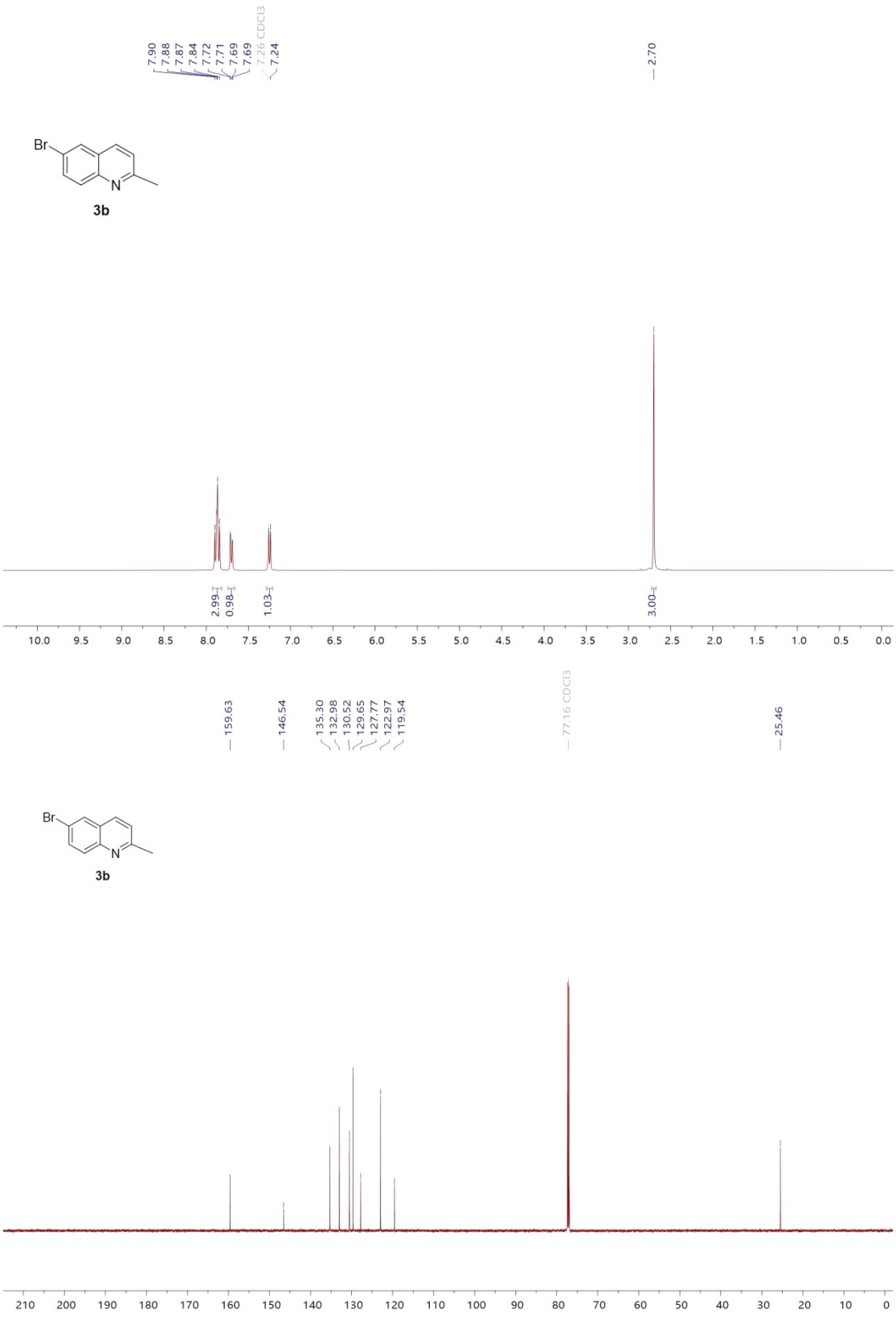

Quinoline **4b**

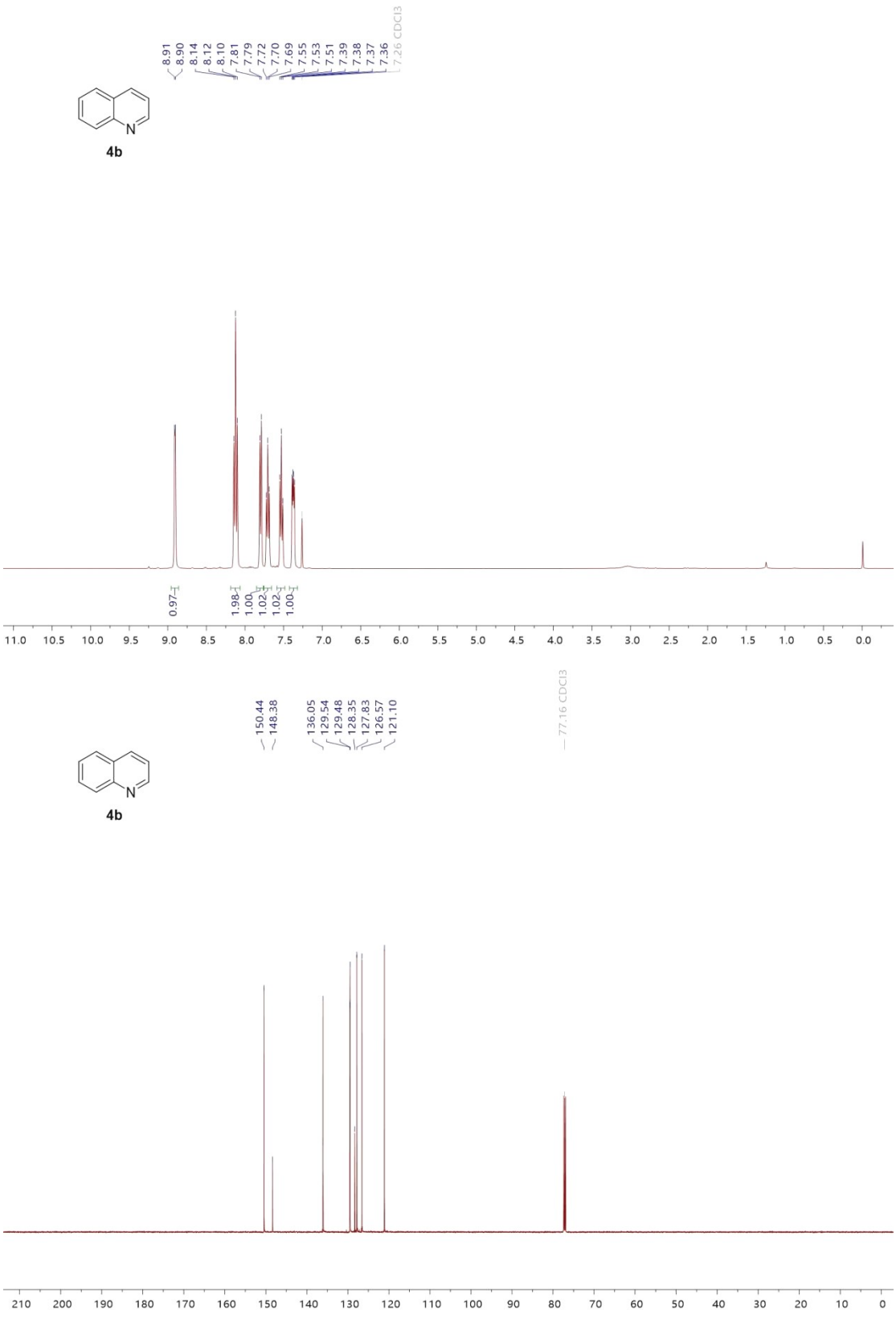

6-Fluoroquinoline **5b**

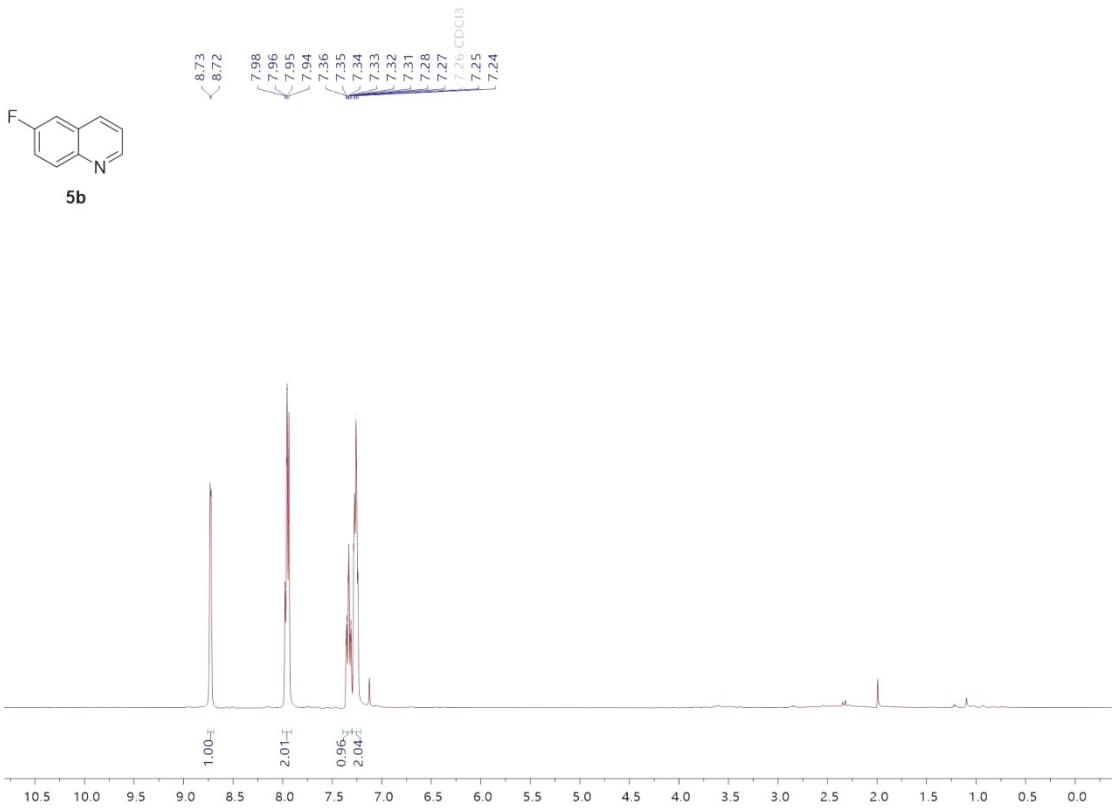

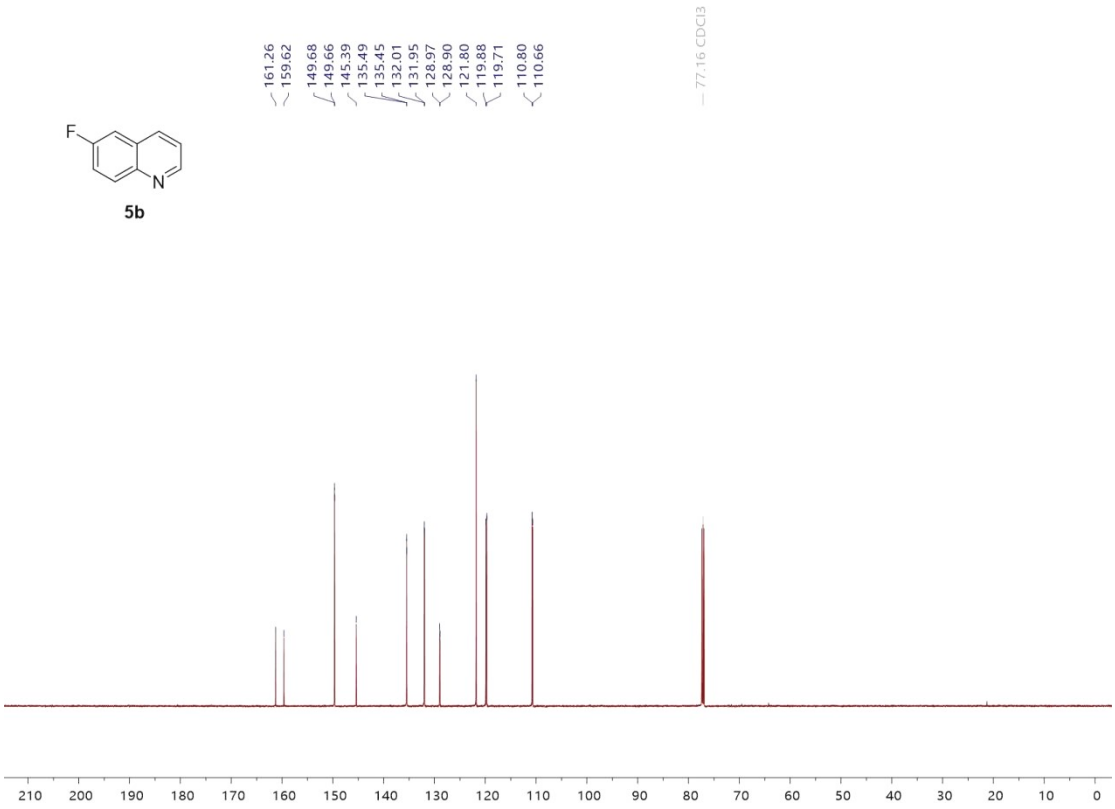

6-Bromoquinoline **6b**

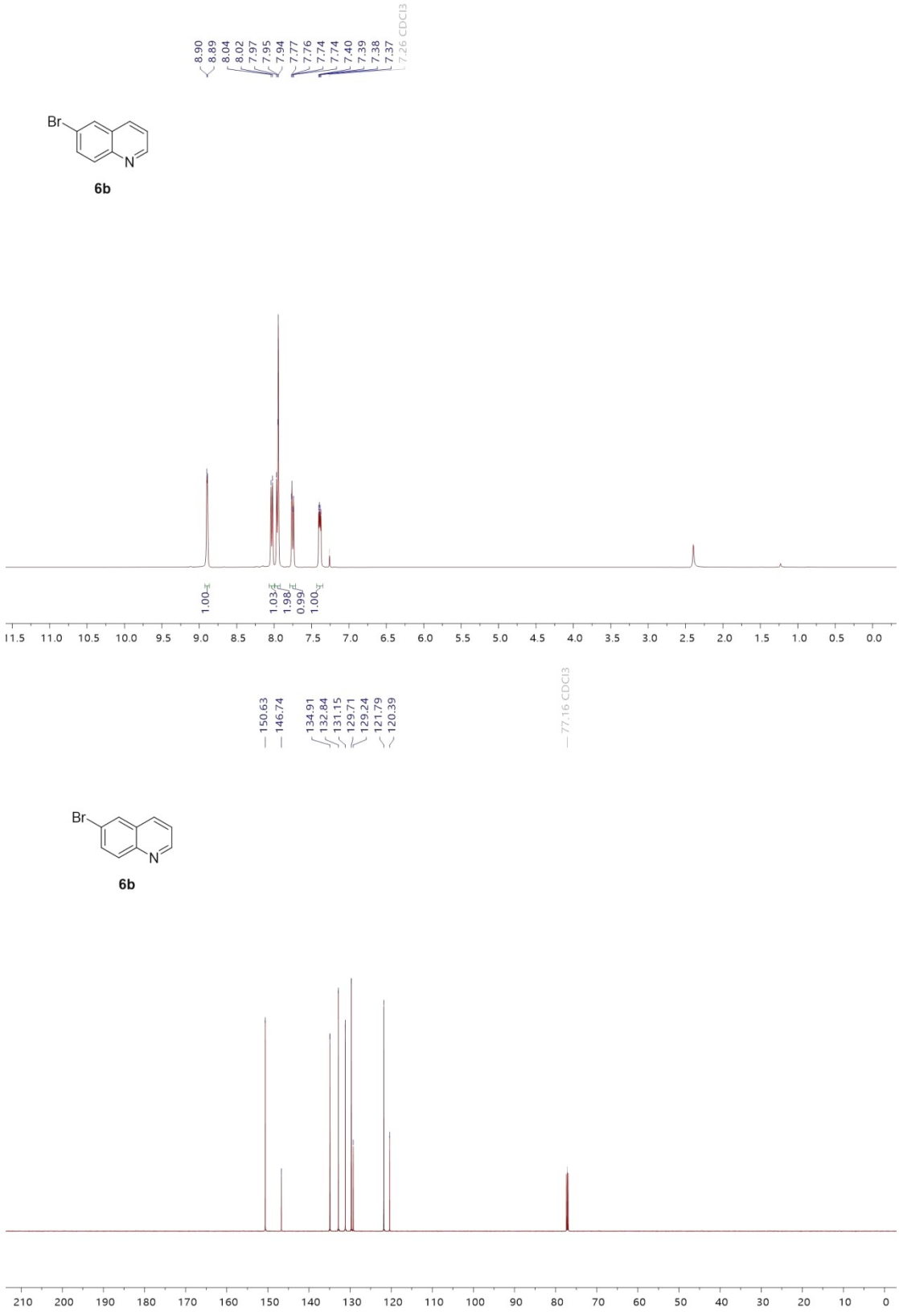

6-Chloroquinoline **7b**

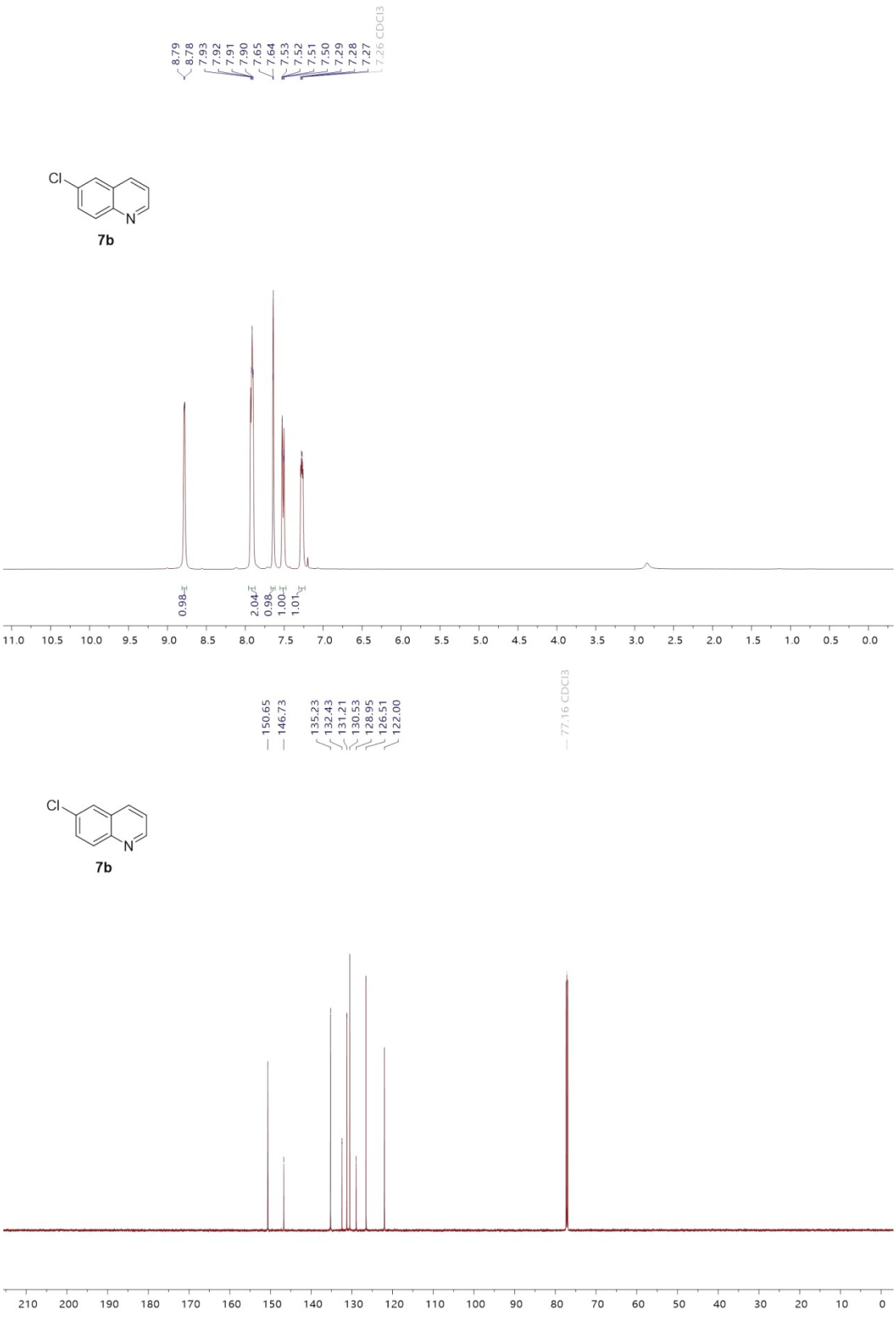

6-Phenylquinoline **8b**

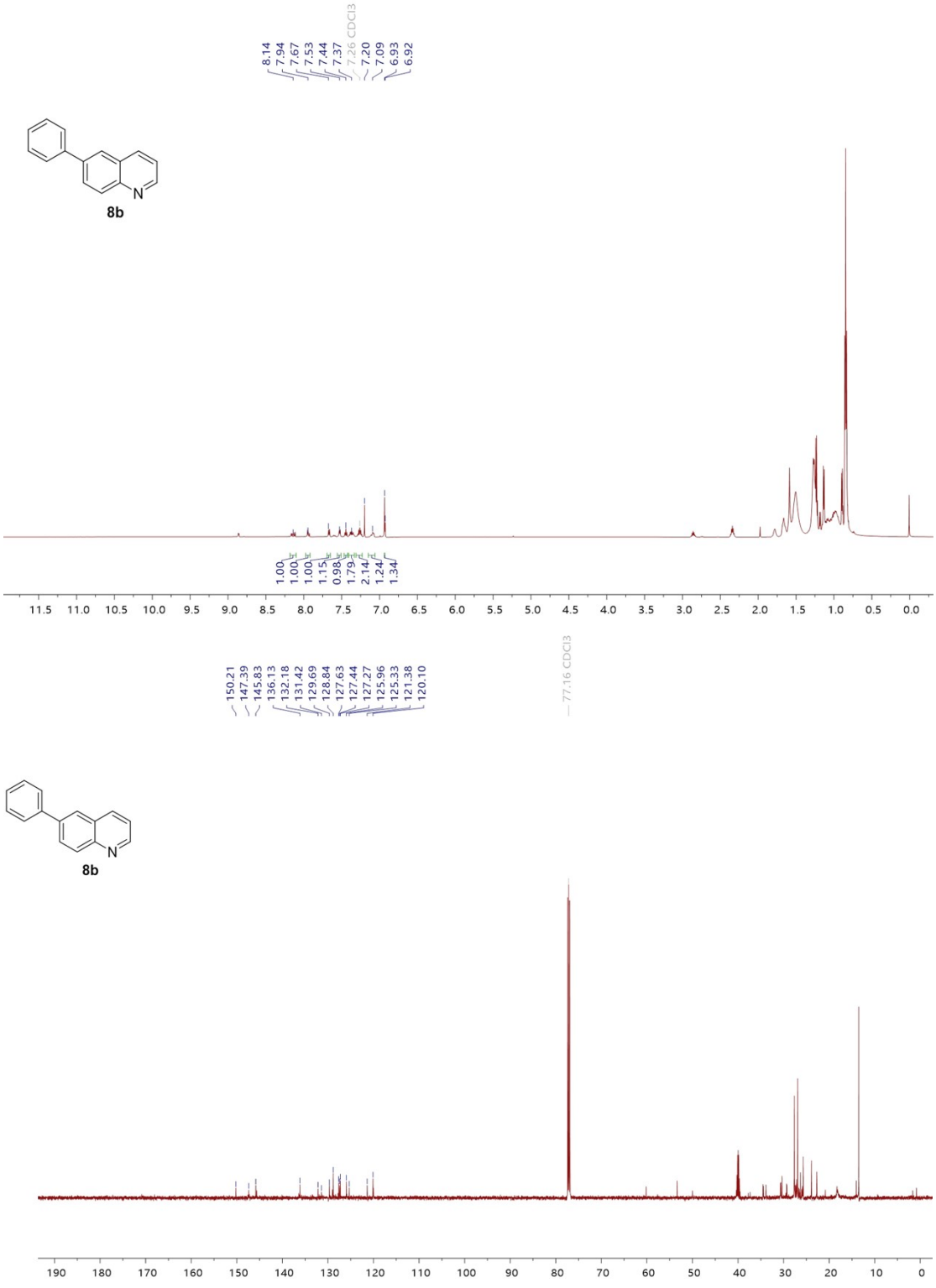

6-Methoxyquinoline **9b**

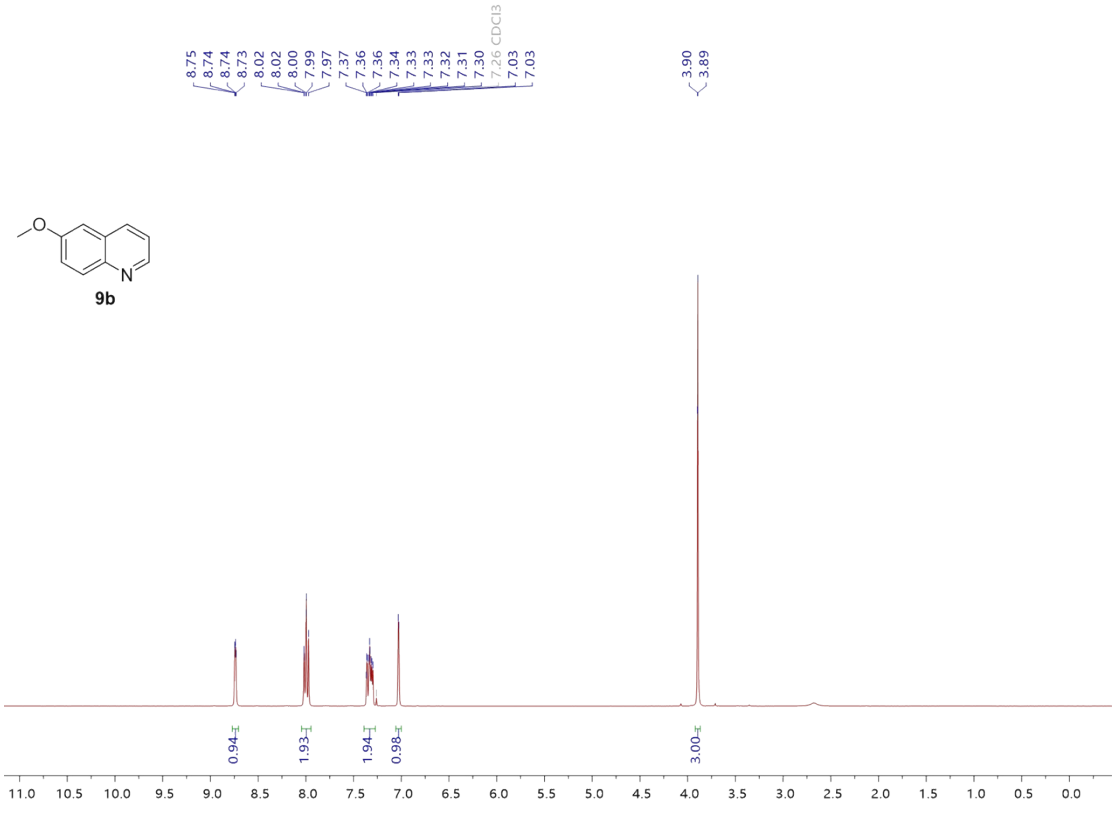

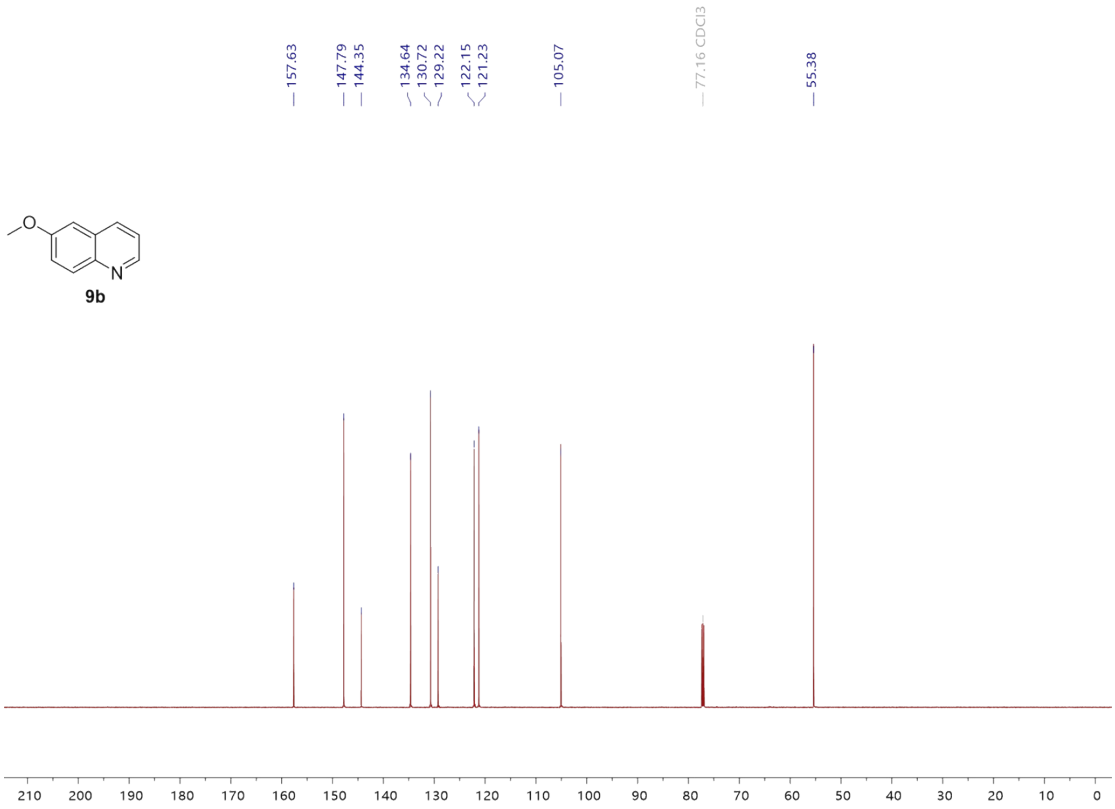

6-Hydroxyquinoline **10b**

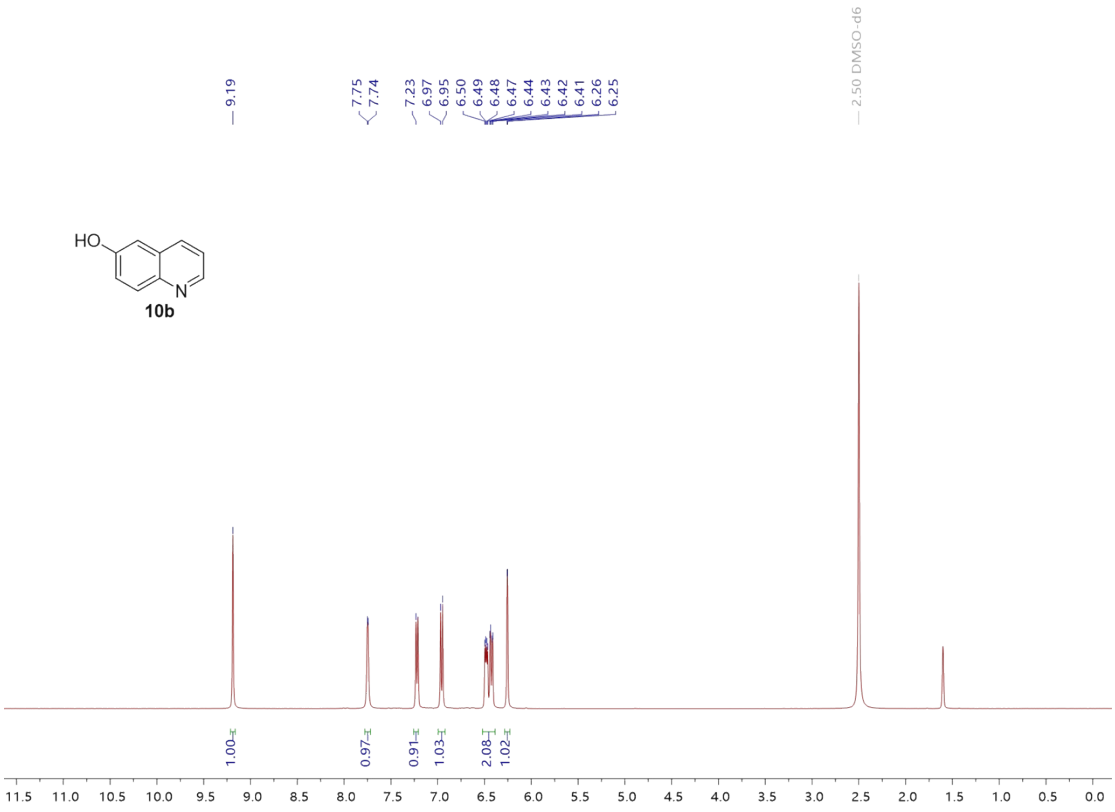

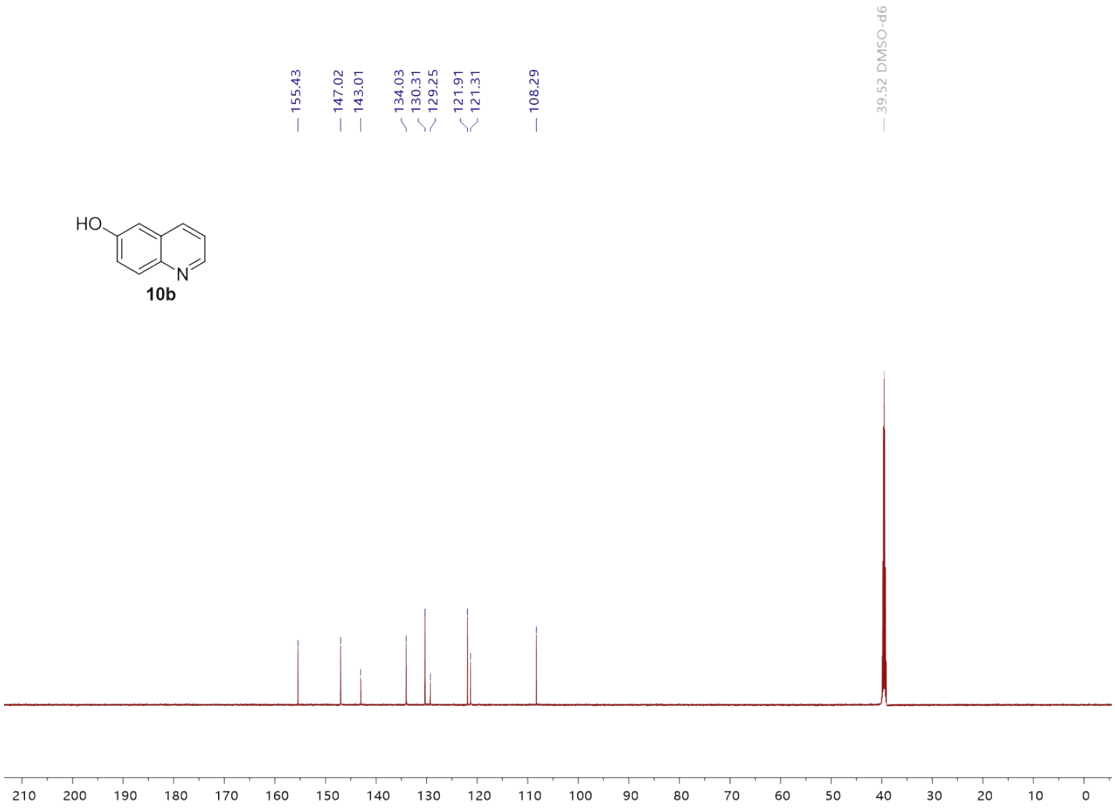

3-Methylquinoline **11b**

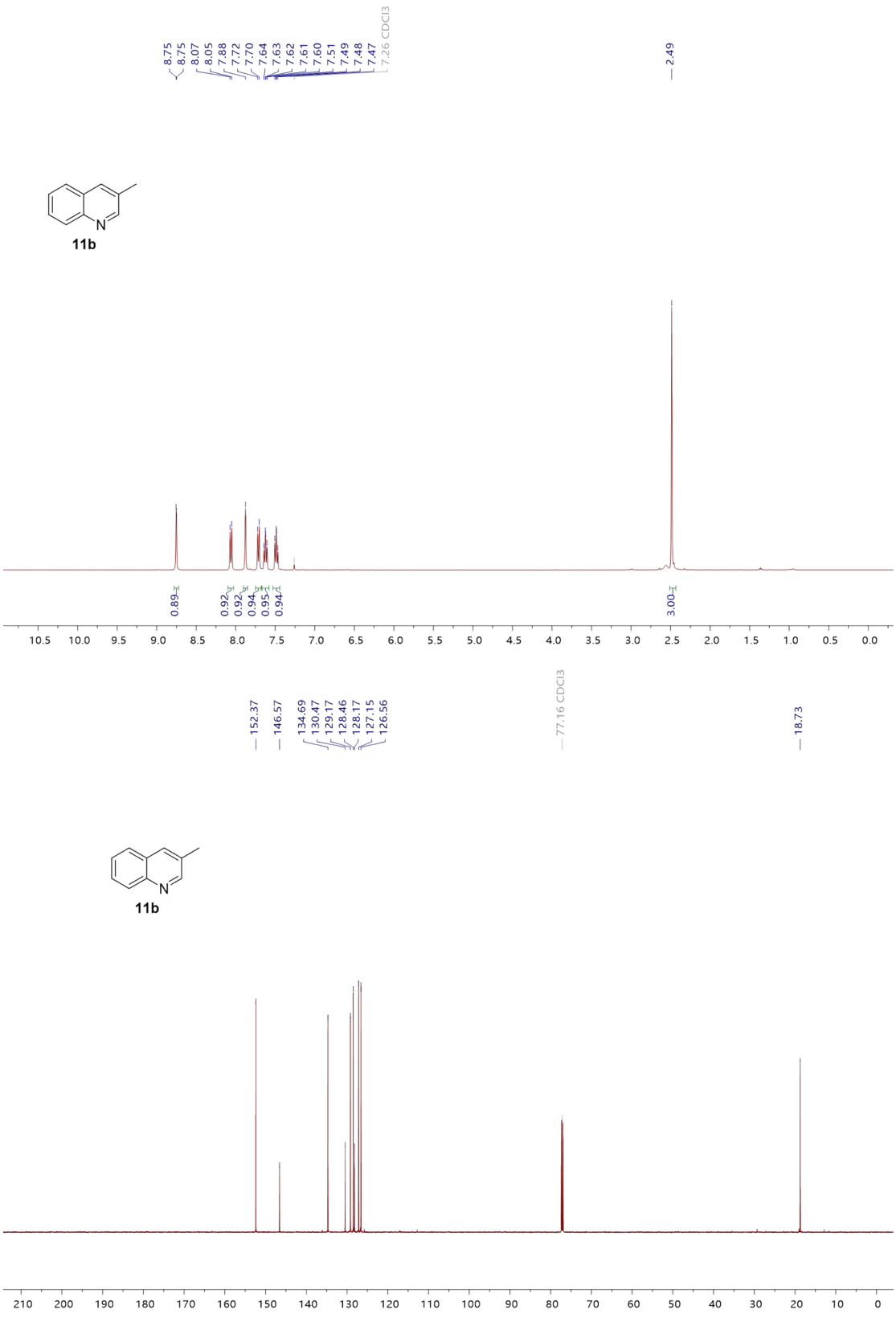

4-Methylquinoline **12b**

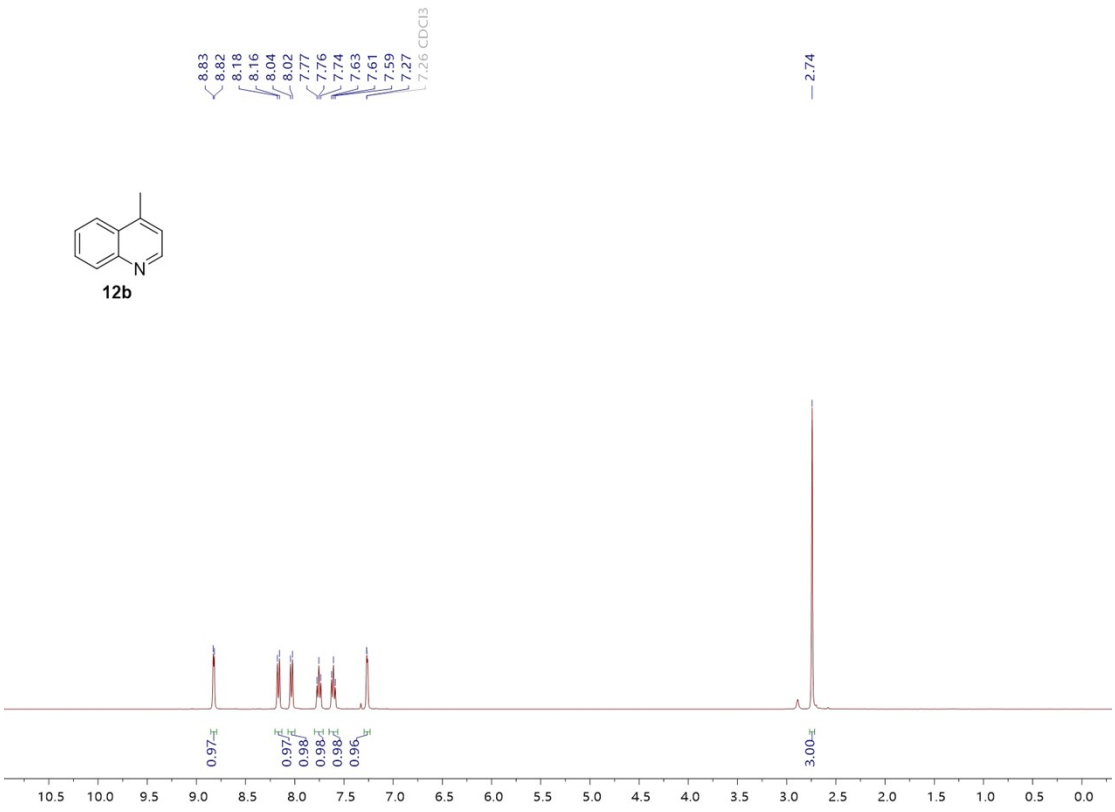

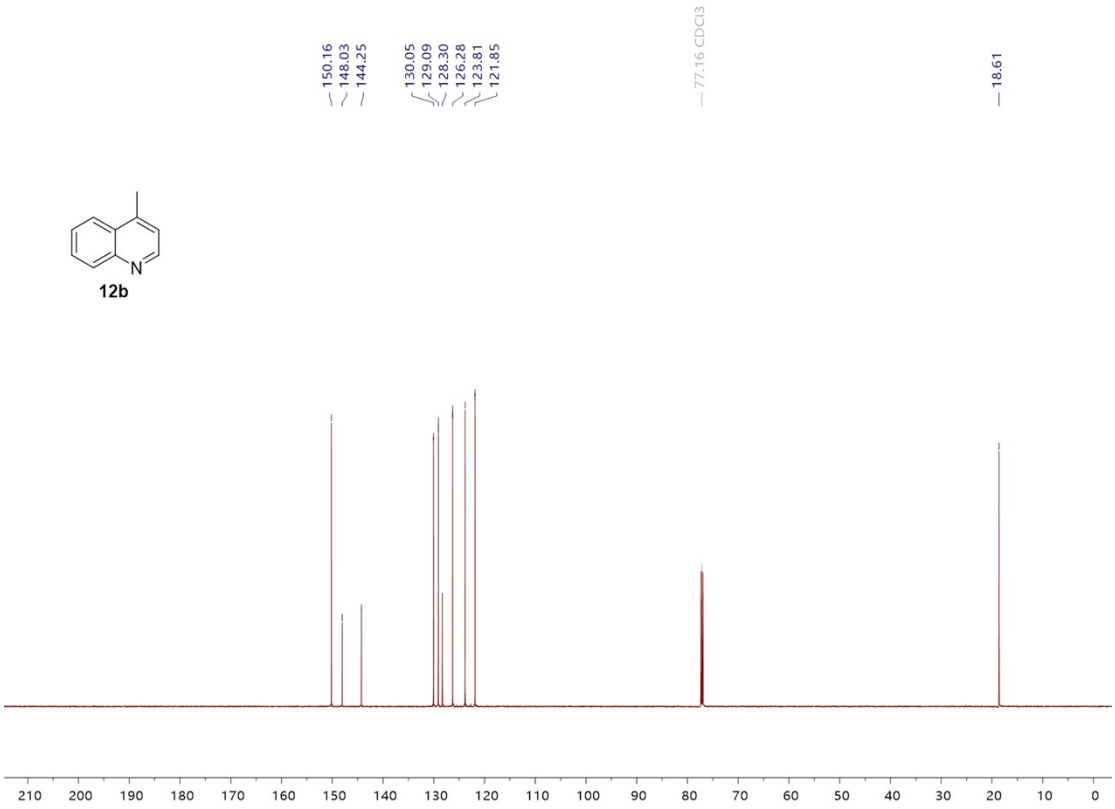

5-Methylquinoline **13b**

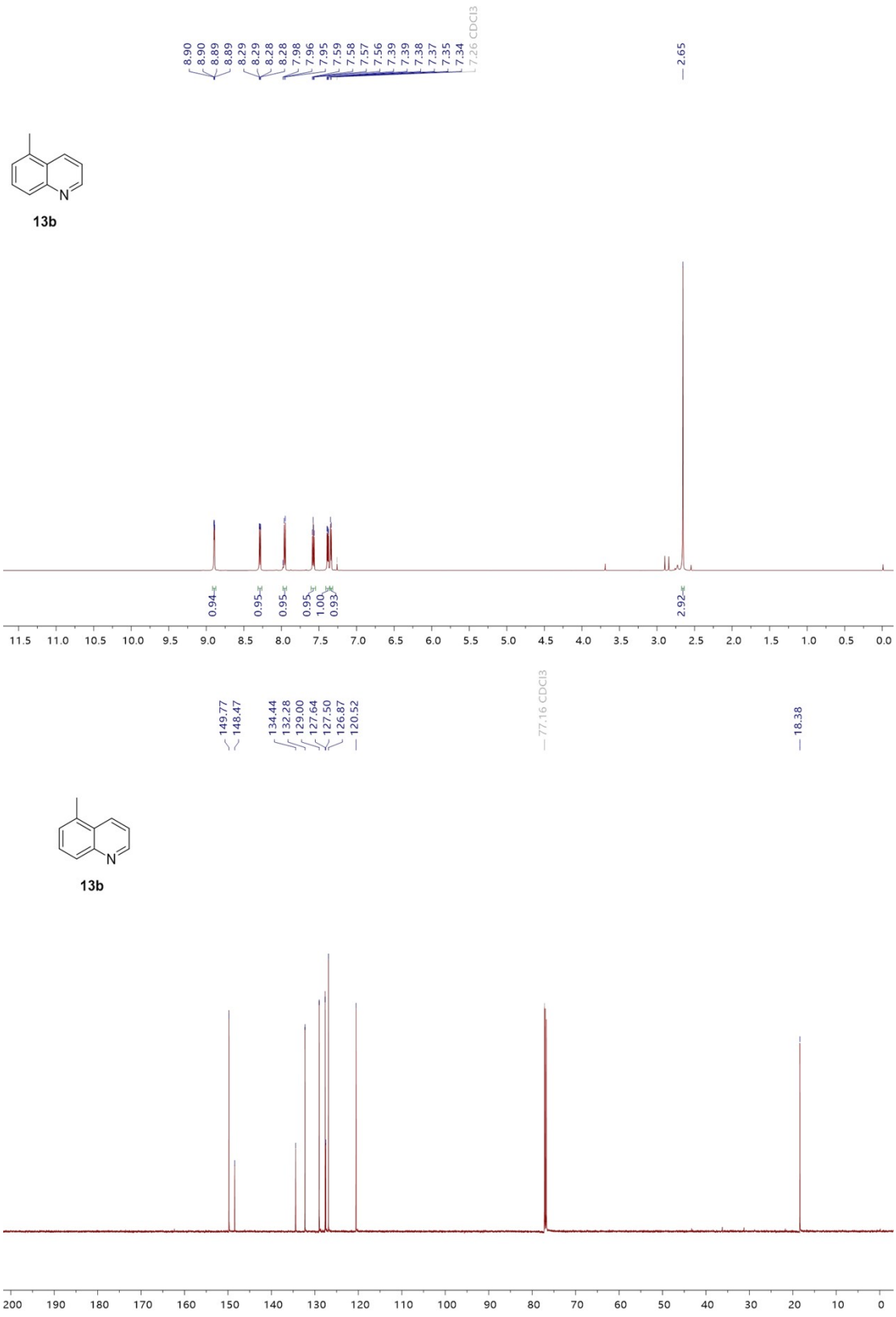

6-Methylquinoline **14b**

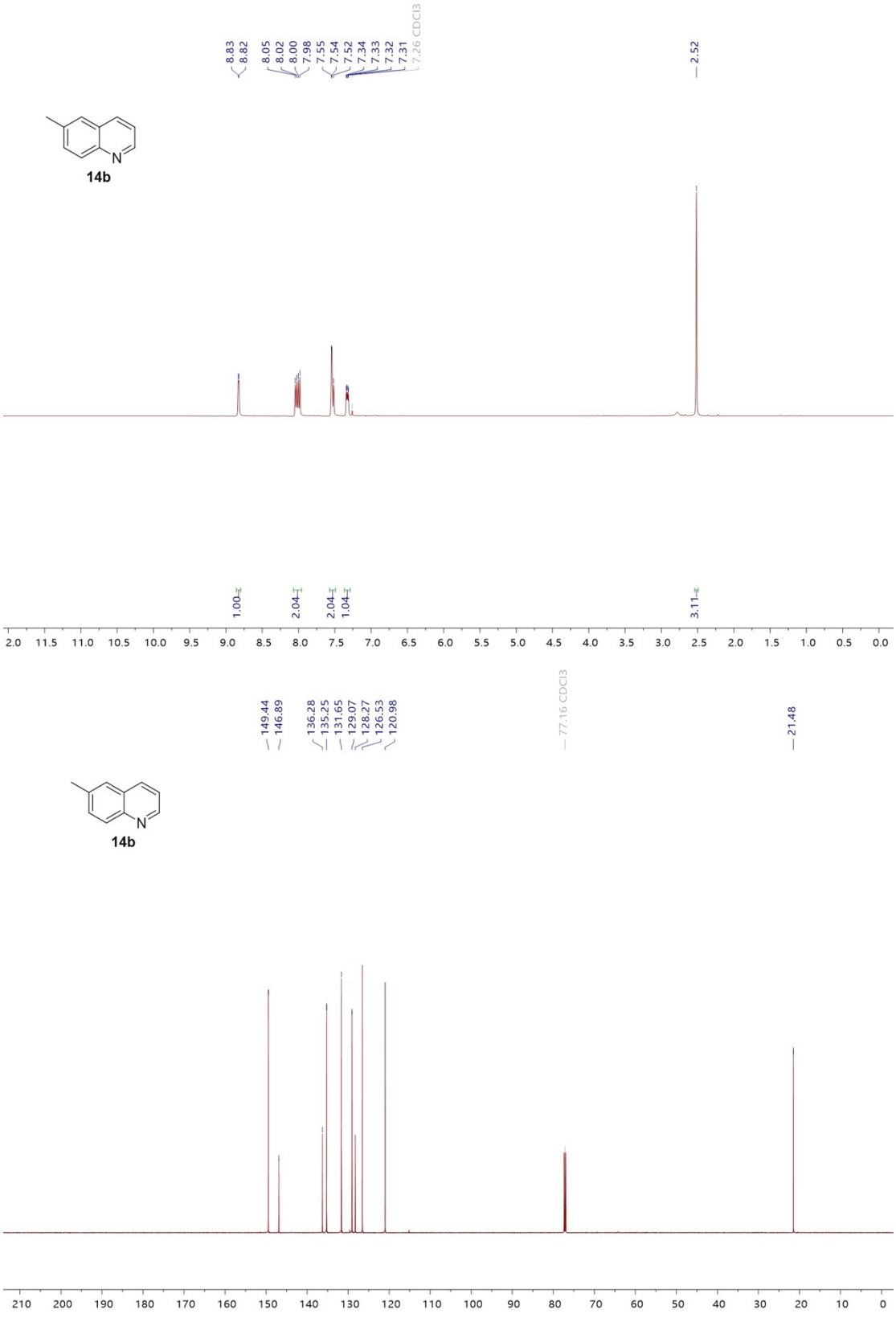

7-Methylquinoline **15b**

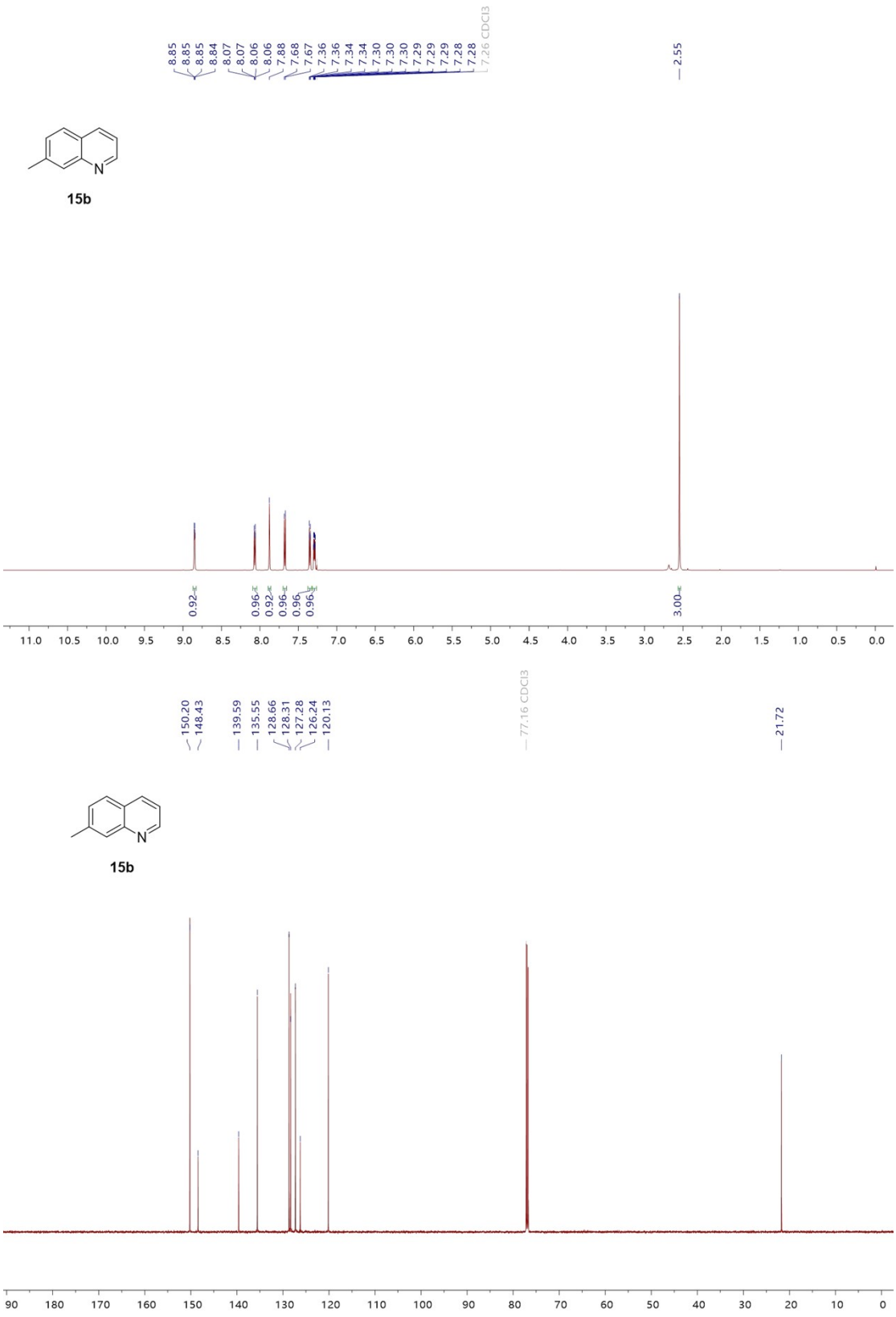

8-Methylquinoline **16b**

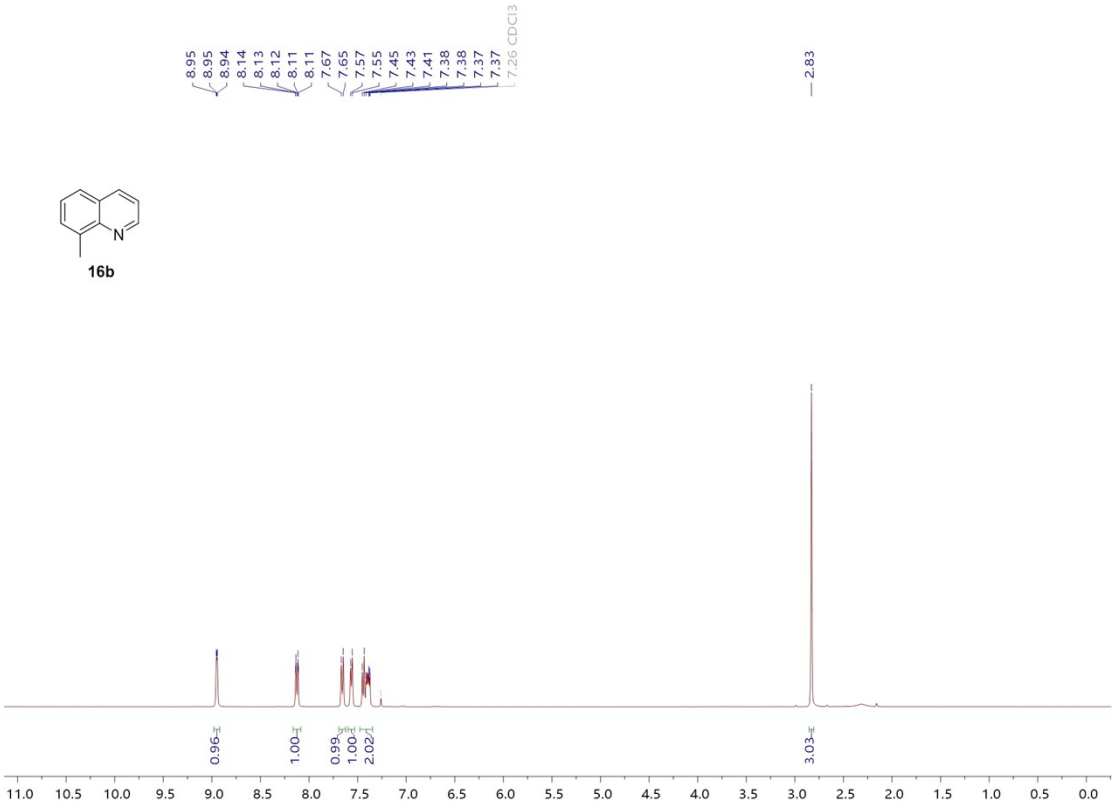

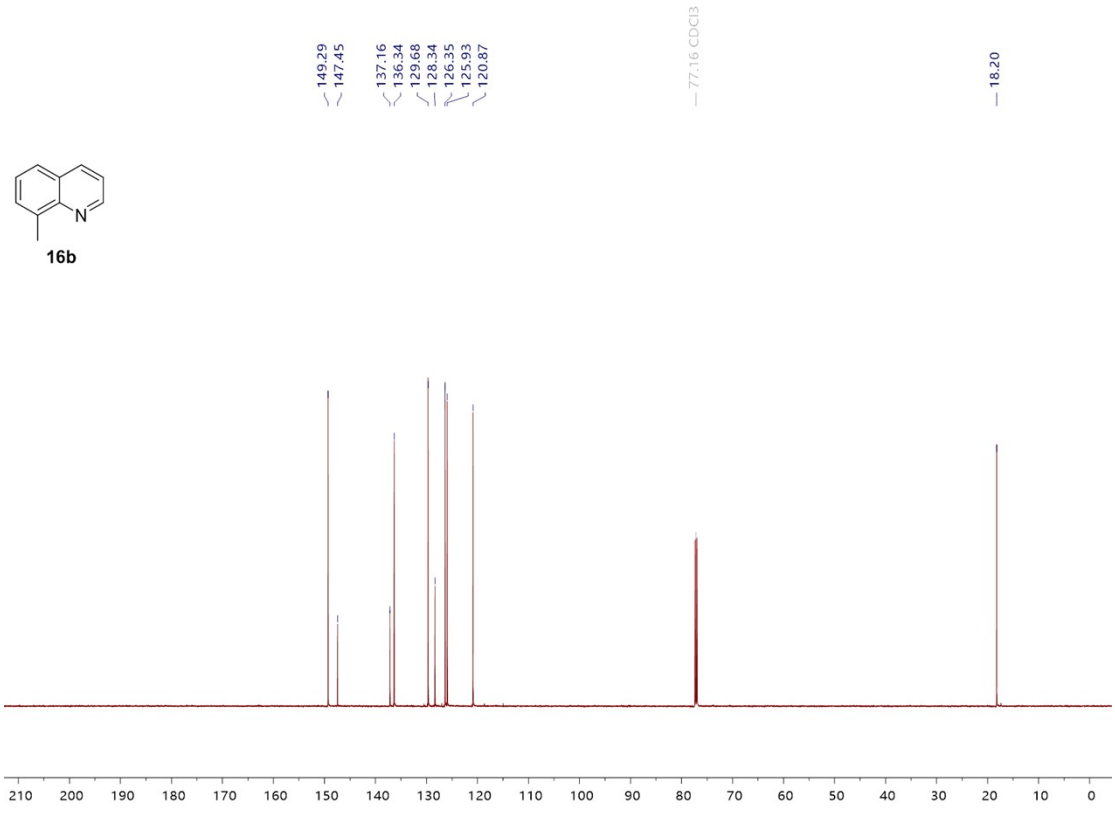

7-Methoxyquinoline **17b**

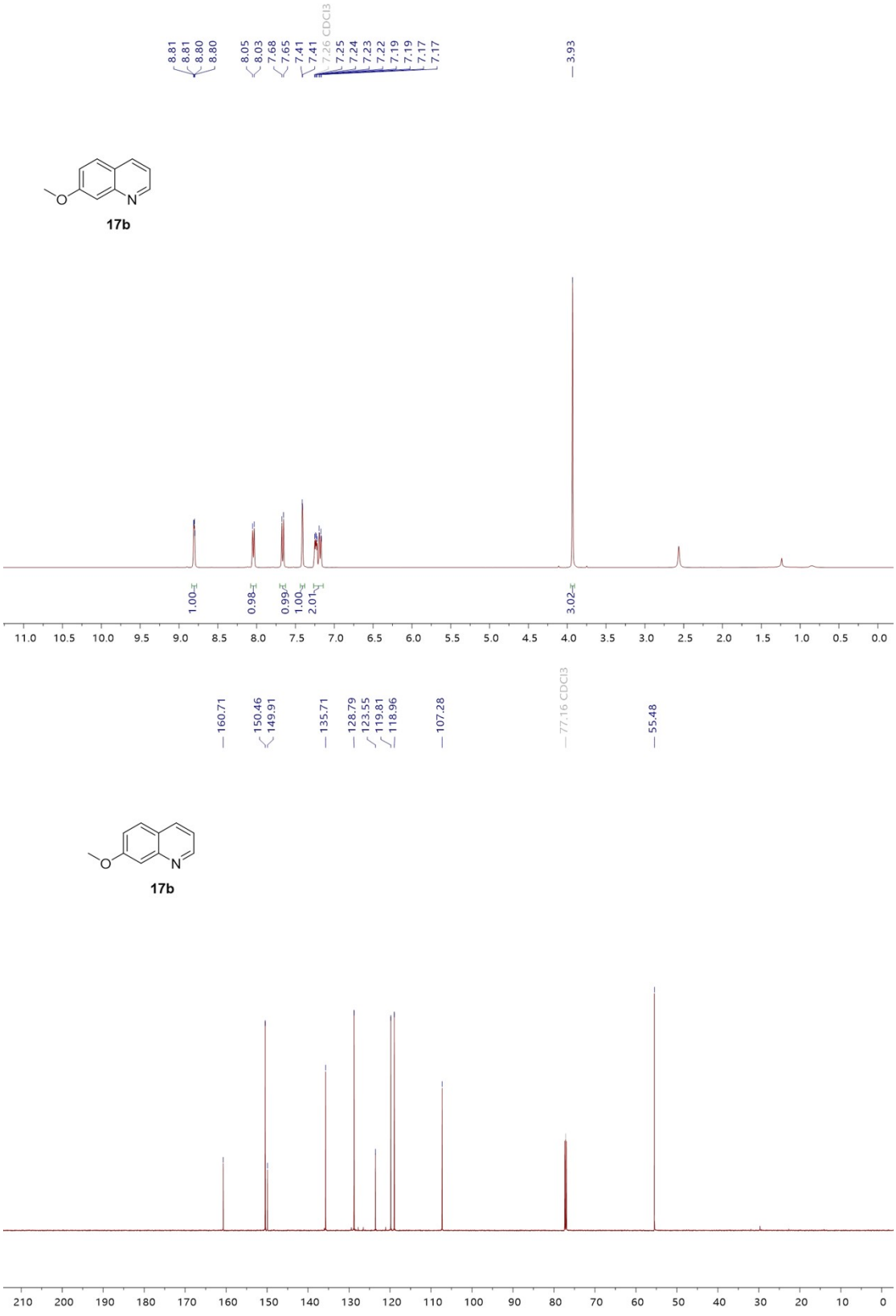

7-Chloroquinoline **18b**

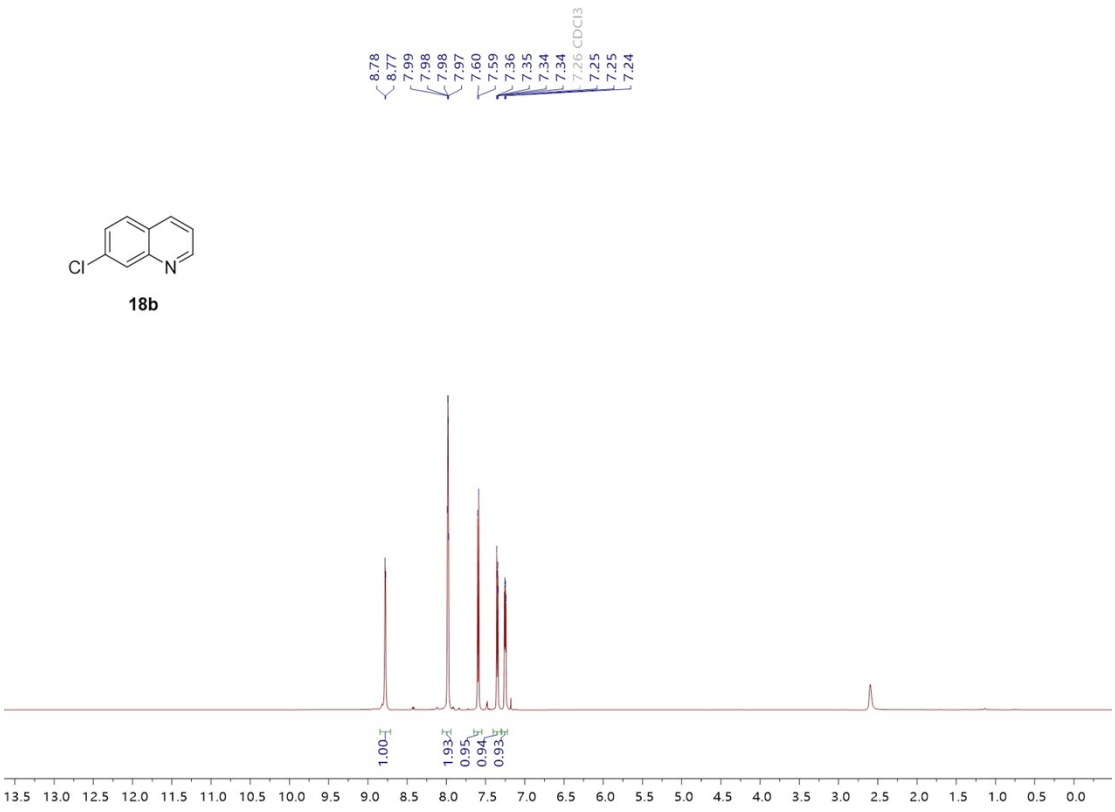

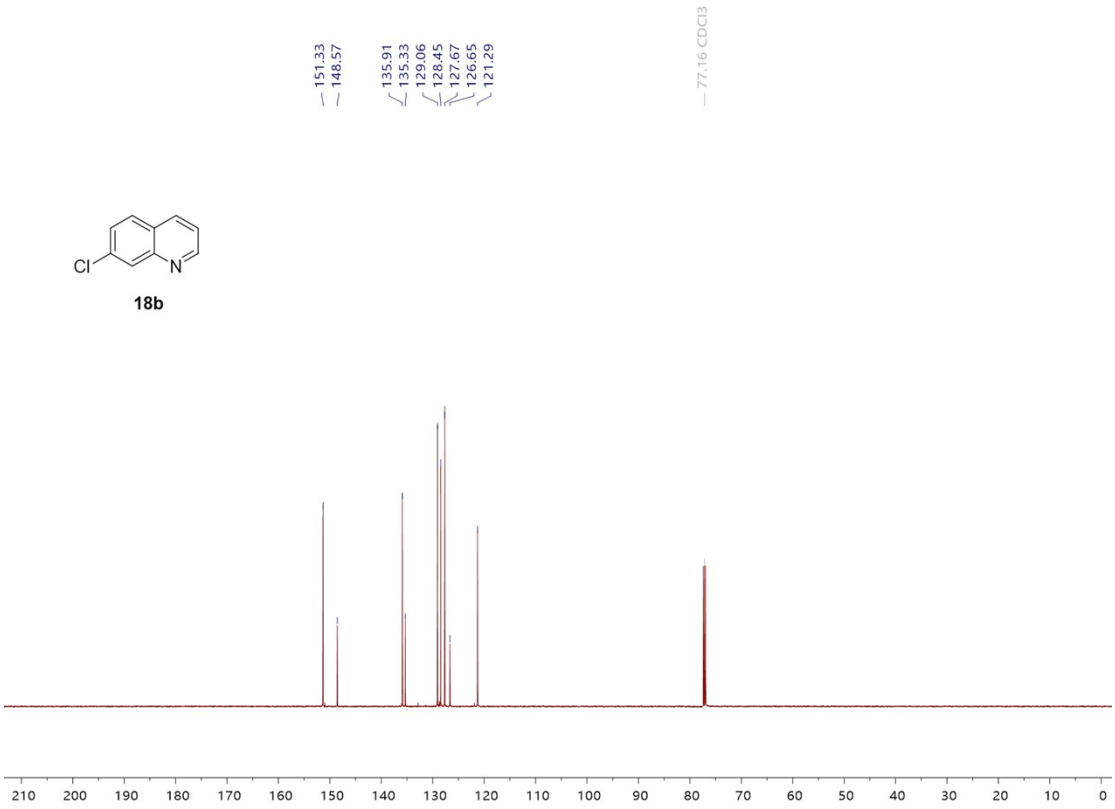

7-Bromoquinoline **19b**

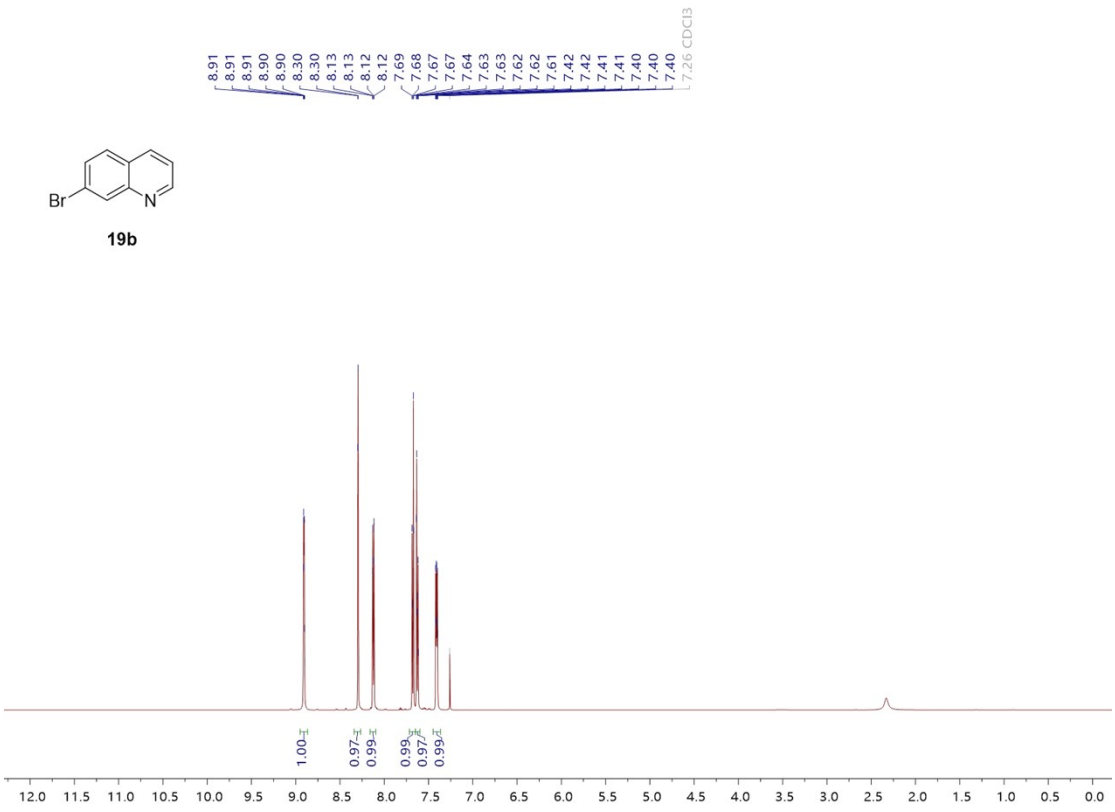

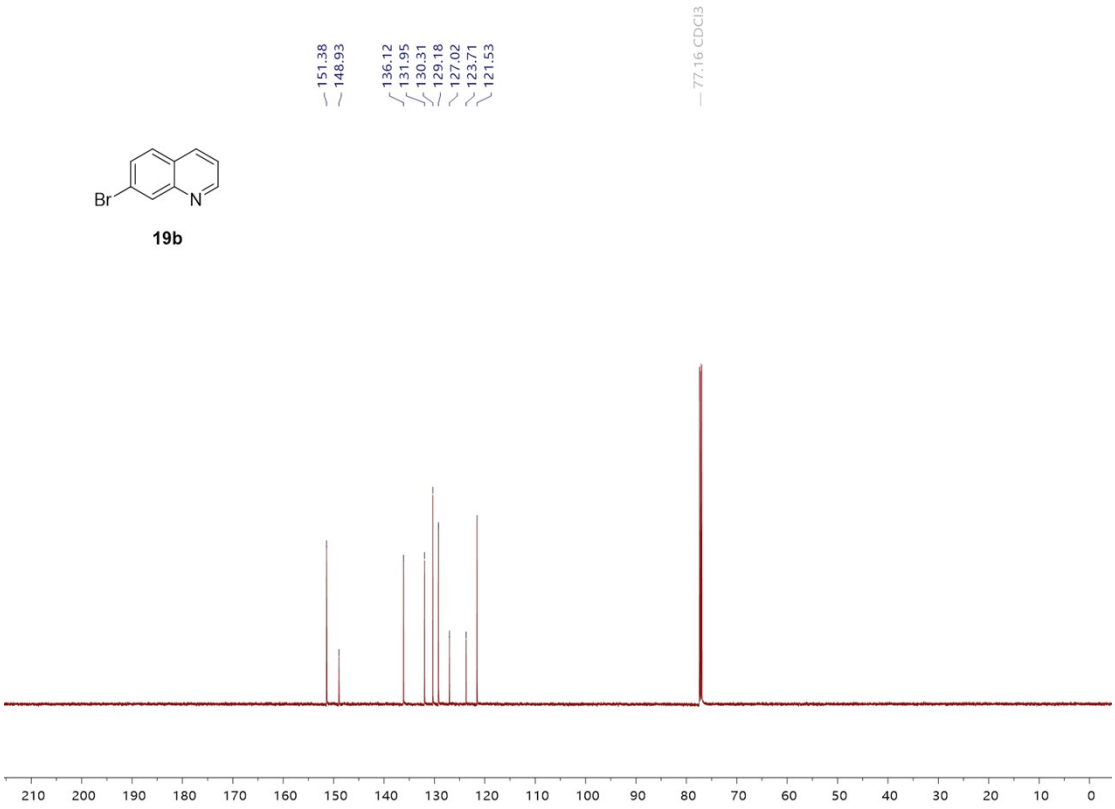

4-Hydroxyquinoline **20b**

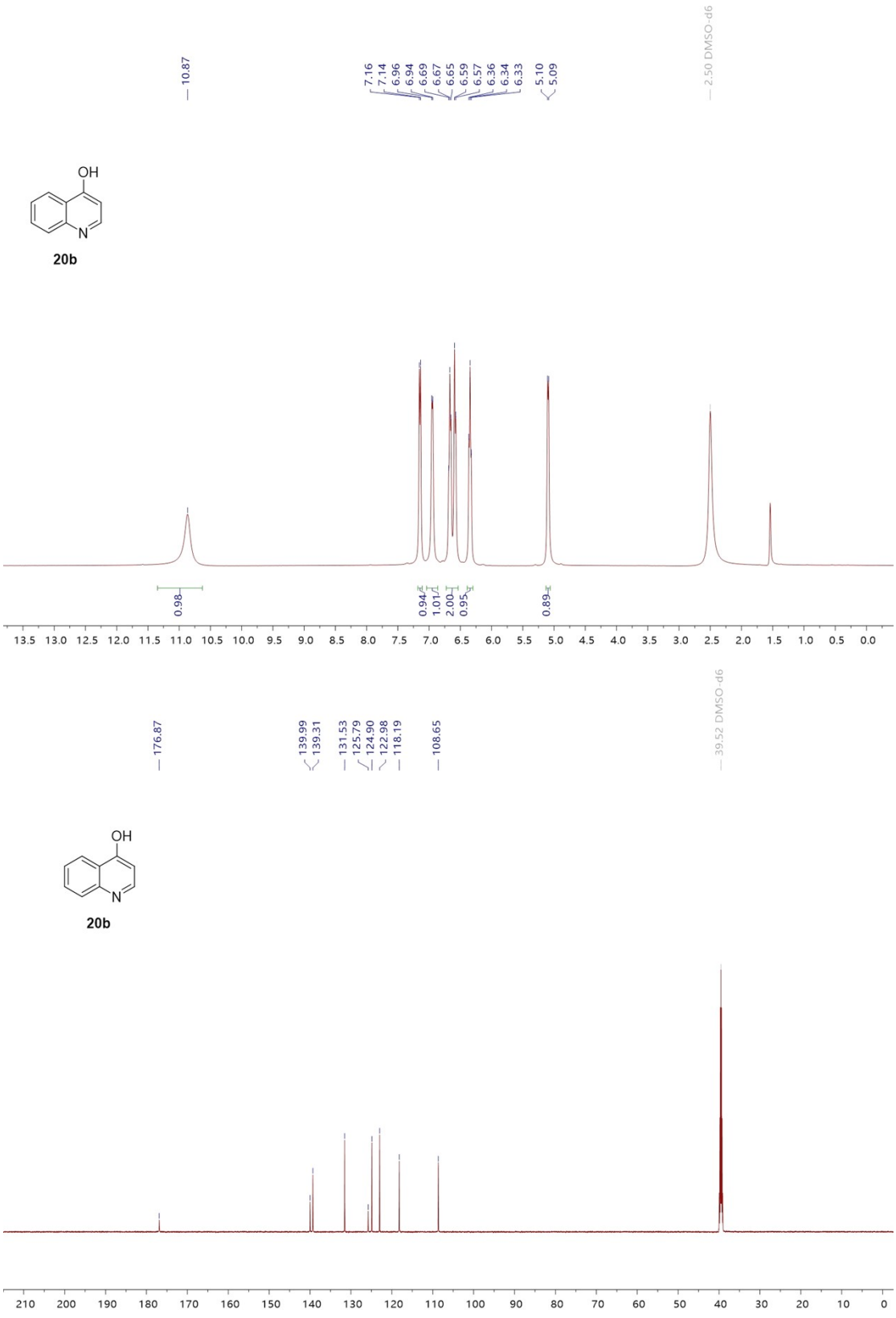

8-Hydroxyquinoline **21b**

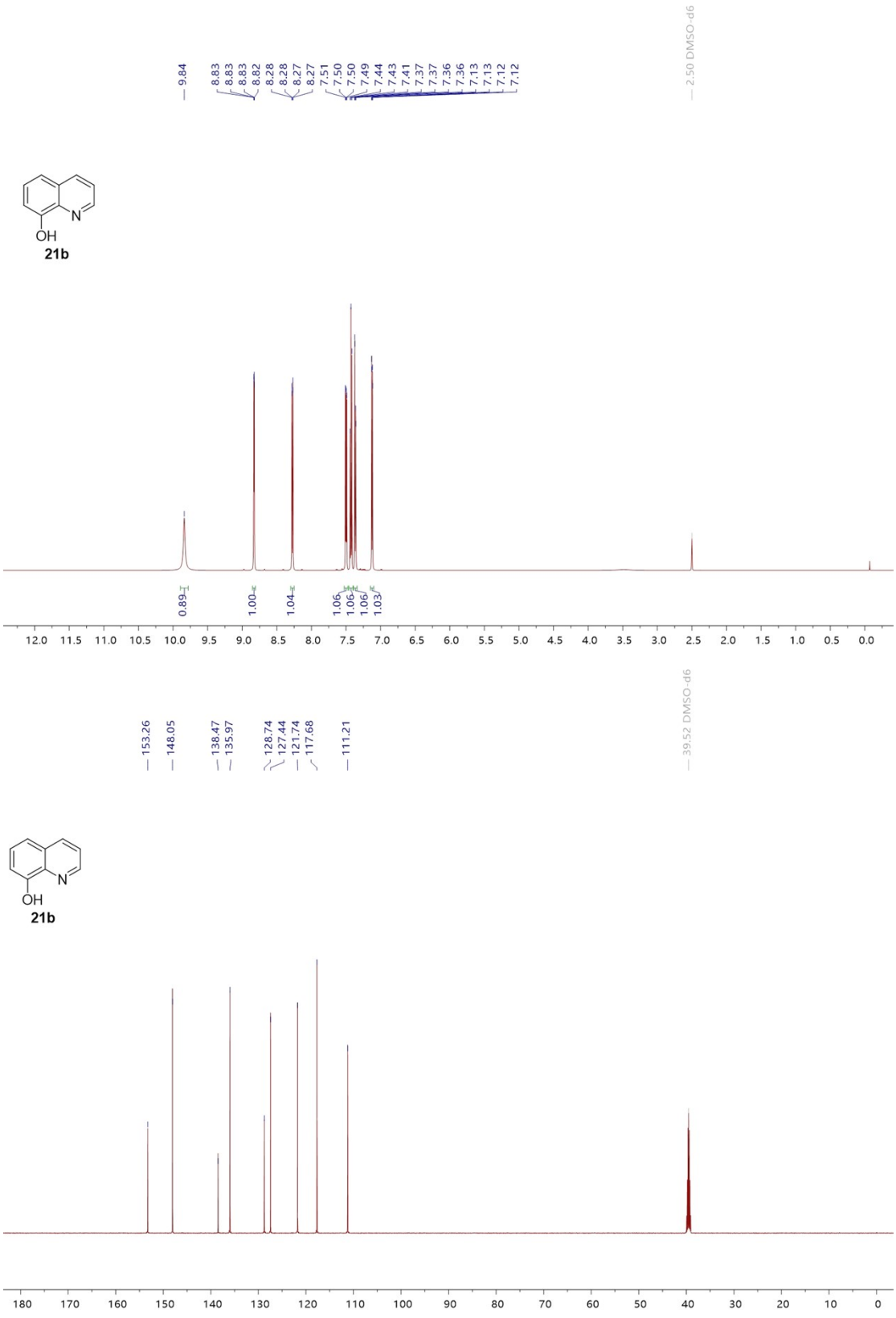

6-Bromo-4-Methylquinoline **22b**

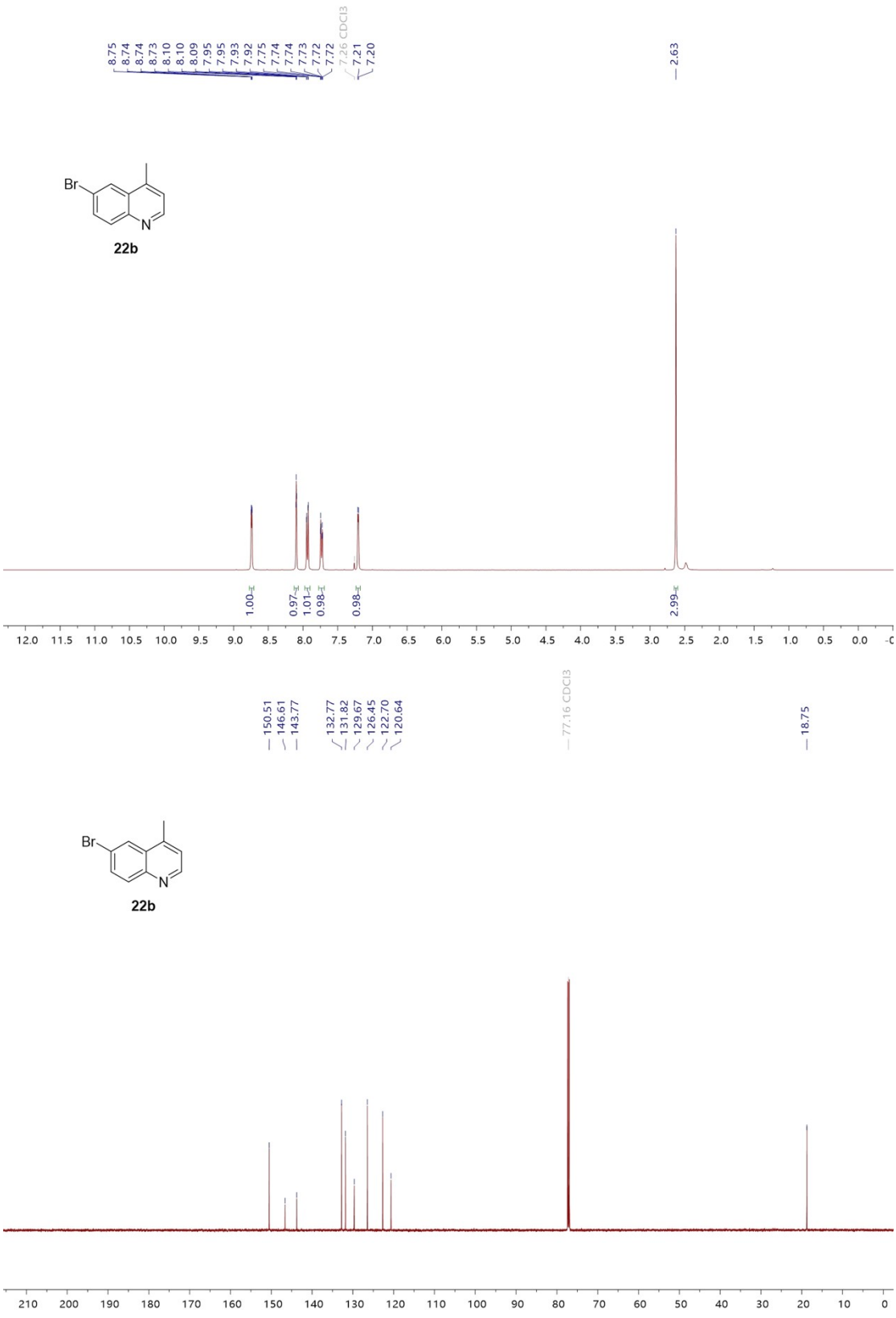

1-Methylisoquinoline **23b**

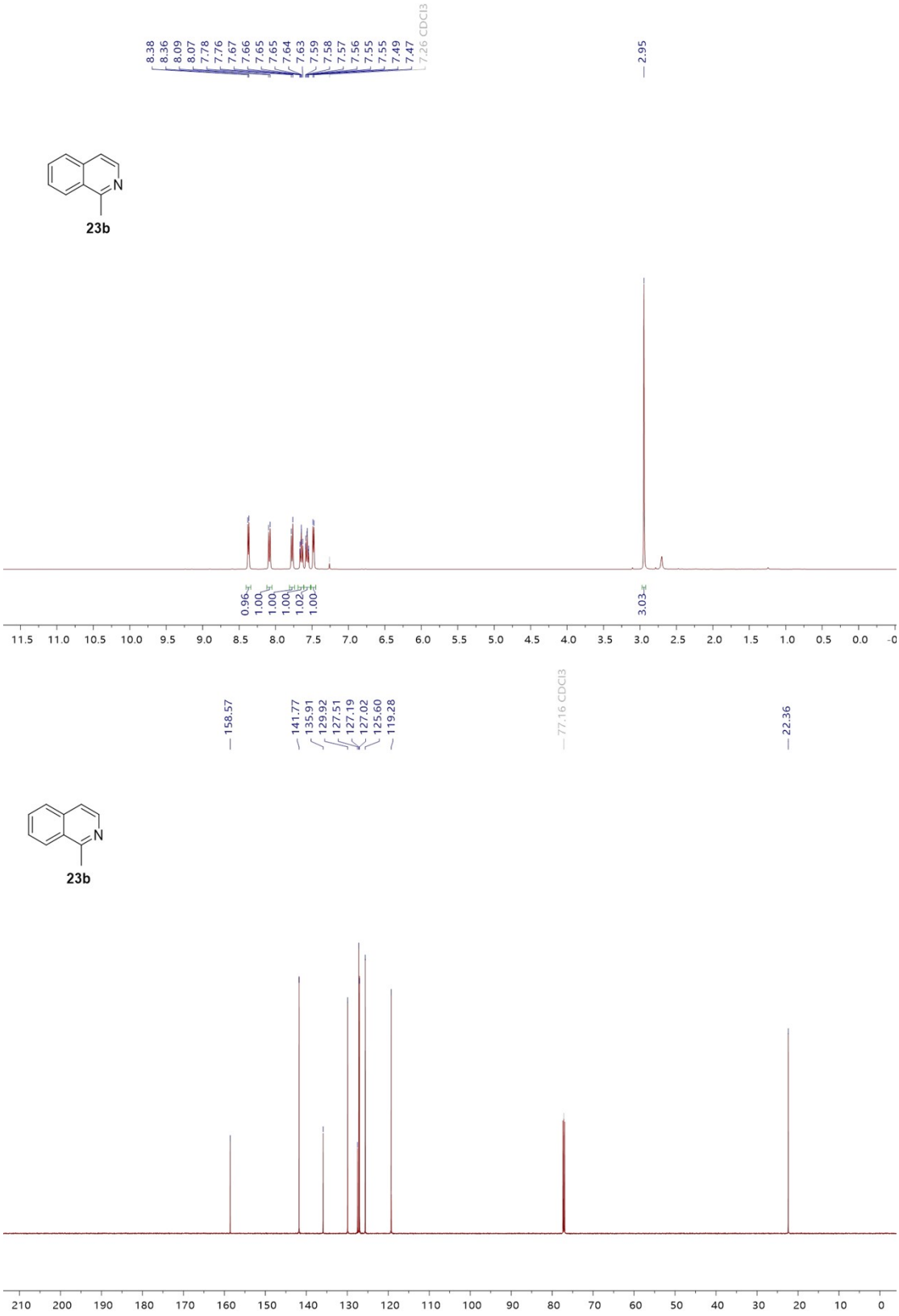

1-Phenylisoquinoline **24b**

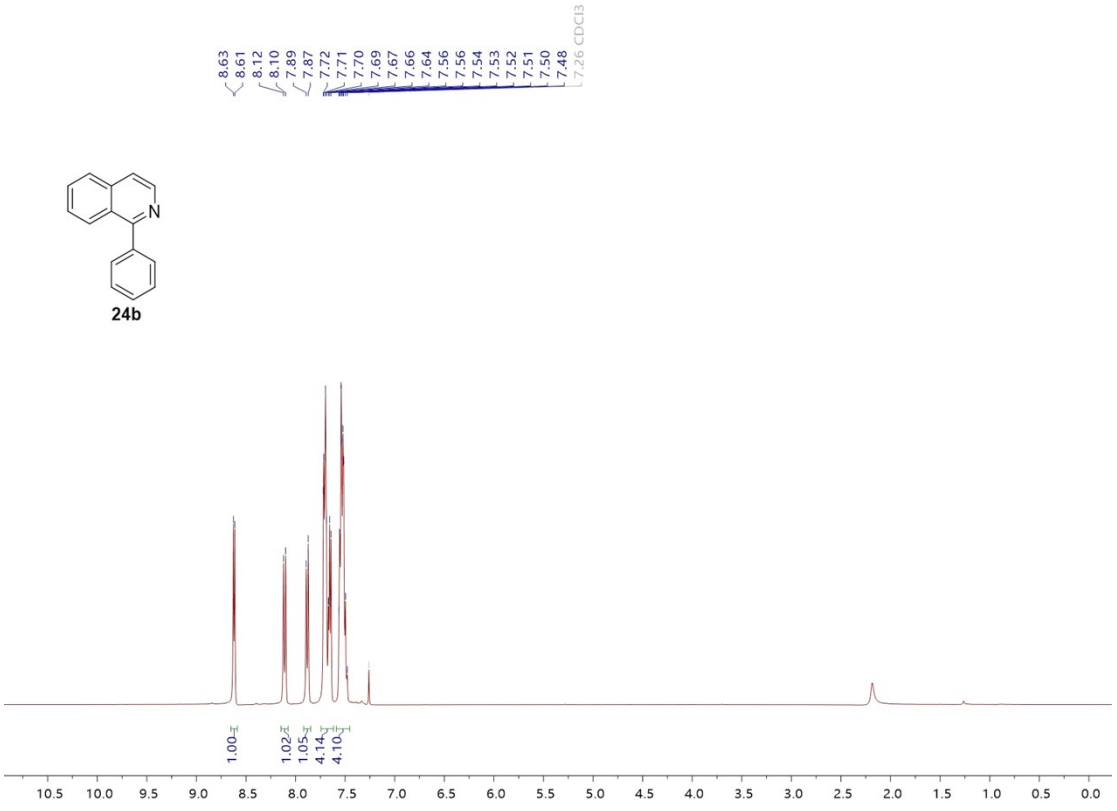
8.63
8.61
8.12
8.10
7.89
7.87
7.72
7.71
7.70
7.69
7.67
7.66
7.64
7.56
7.56
7.54
7.53
7.52
7.51
7.50
7.48
7.26 CDCl3
N
24b
1.00
1.02
1.05
4.14
4.10
10.5 10.0 9.5 9.0 8.5 8.0 7.5 7.0 6.5 6.0 5.5 5.0 4.5 4.0 3.5 3.0 2.5 2.0 1.5 1.0 0.5 0.0

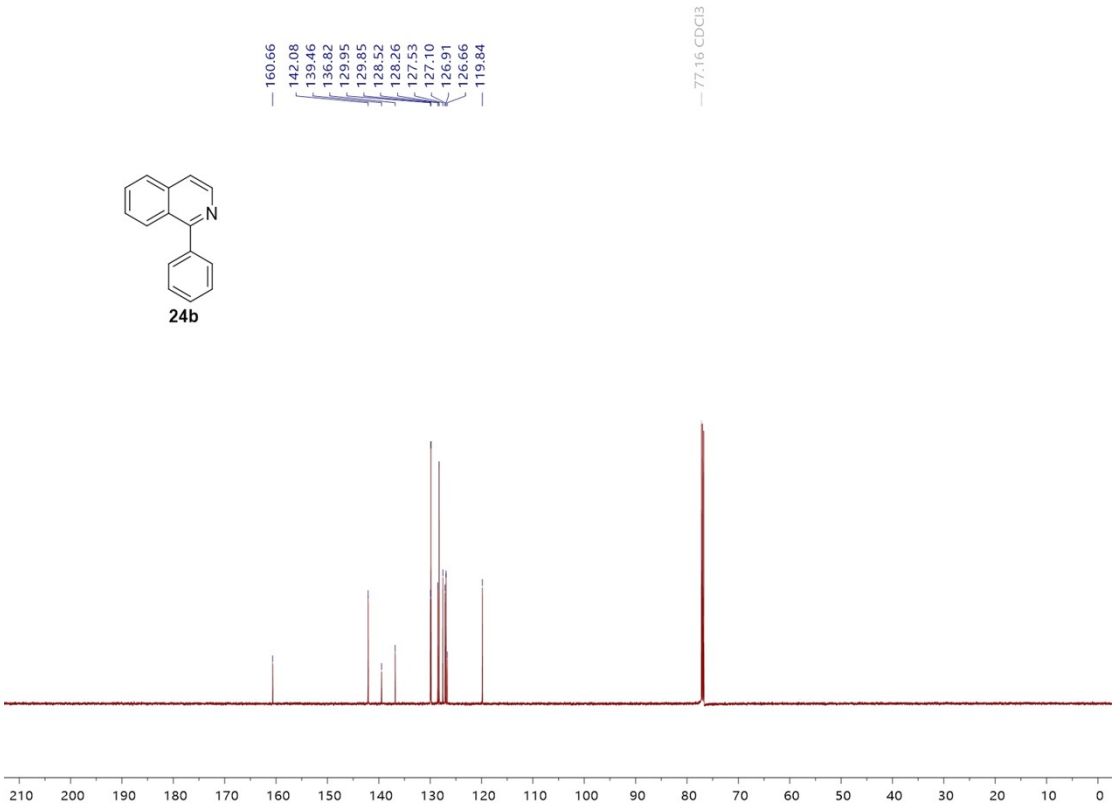
160.66
142.08
139.46
136.82
129.95
129.85
128.52
128.26
127.53
127.10
126.91
126.66
119.84
77.16 CDCl3
N
24b
210 200 190 180 170 160 150 140 130 120 110 100 90 80 70 60 50 40 30 20 10 0

Reference

1. M. Hebditch, M. A. Carballo-Amador, S. Charonis, R. Curtis, J. Warwicker, *Bioinformatics*, 2017, **33** , 3098-3100.
2. G. Deng, N. Wan, L. Qin, B. Cui, M. An, W. Han, Y. Chen, *ChemCatChem*, 2018, **10**, 2374-2377.
3. S. Bera, A. Ber, *Org. Lett.*, 2020, **22**, 6458-6463.
4. G. Jaiswal, M. Subaramanian, M. K. Sahoo, E. Balaraman, *ChemCatChem*, 2019, **11**, 2449-2457.
5. K. Sun, H. Shan, R. Ma, P. Wang, H. Neumann, G.-P. Lu, M. Beller, *Chem. Sci.*, 2022, **13**, 6865-6872.
6. C. Liao, X. Li, K. Yao, Z. Yuan, Q. Chi, Z. Zhang, *ACS Sustainable Chem. Eng.*, 2019, **7**, 13646-13654.
7. T. Liu, K. Wu, L. Wang, Z. Yu, *Adv. Synth. Catal.*, 2019, **361**, 3958-3964.